Journal of Petroleum Science and Engineering 169 (2018) 317–336

Contents lists available at ScienceDirect

Journal of Petroleum Science and Engineering

journal homepage: www.elsevier.com/locate/petrol

Development of a fully implicit approach with intensive variables for compositional reservoir simulation

Bruno Ramon Batista Fernandes[a], Francisco Marcondes[b,*], Kamy Sepehrnoori[a]

[a] Department of Petroleum and Geosystems Engineering, The University of Texas at Austin, Austin, USA
[b] Department of Metallurgical Engineering and Material Science, Federal University of Ceará, Fortaleza, Brazil

ARTICLE INFO

Keywords:
Compositional reservoir simulation
IMPEC
Fully implicit
Finite volume method
CO_2 flooding

ABSTRACT

Compositional reservoir simulators are important tools for application in enhanced oil recovery processes. These simulators solve partial differential equations arising from modeling fluid flow in permeable media. Various algorithms for the solution of such partial differential equations are available, which their application greatly impacts the computational performance of the simulators. In this work, a new fully implicit approach called PZS (pressure, overall composition, and water saturation) is proposed and implemented. The new formulation considers pressure, water saturation, and overall compositions as primary variables, reducing the number of unknowns by one when compared to other volume balance fully implicit formulations. The new approach is obtained by a variable change and elimination of a well known volume balance approach. The new approach is implemented in the UTOMPRS simulator that has been developed at The University of Texas at Austin for simulation of several multicomponent/multiphase recovery processes. The PZS formulation is compared to the volume balance based and IMPEC (Implicit Pressure Explicit Composition) formulations in UTCOMPRS. We observe that the PZS approach is, in general, faster than the other approaches tested.

1. Introduction

Reservoir simulators are tools developed to simulate fluid flow in porous media. In the oil industry, reservoir simulators are used to forecast the oil and gas recoveries, perform field optimization and economic analysis, and assess uncertainties. For such analysis, an extensive amount of simulation is required, which may result in excessive computational effort. Therefore, fast and robust algorithms are essential. In general, fast algorithms are obtained by combining adaptive implicit methods (AIM) with high-performance computing techniques. Adaptive implicit methods are obtained by combining a Fully Implicit (FI) formulation with an IMPEC approach. Therefore, the performance of an AIM approach is limited by the performance of each formulations.

Many formulations have been proposed for compositional reservoir simulation using an Equation of State (EOS). Fussell and Fussell (1979) were the first to propose the use of fugacities and EOS in a reservoir simulator. Their model was based on an IMPEC formulation and the primary variable set changed according to the amount of oil and gas in each gridblock. Coats (1980) proposed a FI method that became well known as the natural variable formulation. In this formulation, Coats (1980) considered the pressure, saturations, and phase compositions as primary variables; therefore, the set of primary variables will also change as the phases present in a gridblock change. The natural variable formulation has the advantage of requiring the solution of one less equation per gridblock for the linear system, arising from discretization of governing partial differential equations modeling fluid flow in the reservoir, when compared to most of the other FI formulations available in the literature. However, it requires the use of a Gaussian elimination to decouple the equilibrium constraints from the flow equations. Nghiem et al. (1981) developed a new IMPEC-type formulation that differed from all the previous one by allowing the solution of pressure and compositions separately. The approach implemented by Nghiem et al. (1981) is based on the one presented by Kazemi et al. (1978), differing only on weighting factors for the pressure equation, which, according to Wong and Aziz (1989), makes the Jacobian strictly diagonal dominant and symmetric. Young and Stephenson (1983) proposed an IMPEC-type formulation by modifying the primary variable set and the equation ordering proposed by Fussell and Fussell (1979). Chien et al. (1985) presented another FI approach similar to that proposed by Coats (1980), but using the equilibrium ratios (K-values) as primary variables instead of the gas phase mole fractions. Acs et al. (1985) proposed a new IMPEC-type formulation that had the pressure equation obtained from a Taylor series expansion of the fluid volume and the pore volume. This is a powerful one-iteration formulation that controls

* Corresponding author.
E-mail address: marcondes@ufc.br (F. Marcondes).

https://doi.org/10.1016/j.petrol.2018.05.039
Received 31 January 2018; Received in revised form 24 April 2018; Accepted 13 May 2018
Available online 25 May 2018

Table 1
Summary of important formulations for compositional reservoir simulation.

Formulation	Implicitness degree	Iterative method[a]	Primary variables
Fussel and Fussel (1979)	IMPEC	MVNM	$\{P, \widetilde{N}_g, x_{2g},...,x_{n_cg}\}$ or $\{P, \widetilde{N}_o, x_{2o},...,x_{n_co}\}$
Coats (1980)	FI	NM	$\{P_g, S_o, S_g, x_{3g},...,x_{n_cg}\}$
Nghiem et al. (1981)	IMPEC	NM	$\{P, \widetilde{N}_w, \widetilde{N}_h, z_1,...,z_{n_c}\}$ or $\{P, S_w, \widetilde{N}_h, z_1,...,z_{n_c}\}$
Young and Stephenson (1983)	IMPEC	NM	$\{P, \widetilde{N}_w, \widetilde{N}_h, L_g, z_1,...,z_{n_c-1}\}$
Chien et al. (1985)	FI	NM	$\{P, \widetilde{N}_w, \widetilde{N}_1,...,\widetilde{N}_{n_c}\}$
Ács et al. (1985)	IMPEC	OI	$\{P, \widetilde{N}_w, \widetilde{N}_1,...,\widetilde{N}_{n_c}\}$
Watts (1986)	IMPSAT	SOI	$\{P, S_o, S_g, \widetilde{N}_w, \widetilde{N}_1,...,\widetilde{N}_{n_c}\}$
Quandalle and Savary (1989)	IMPSAT	SOI	$\{P, S_w, S_g, x_{2o},...,x_{n_c-1o}\}$ or $\{P, S_w, S_g, x_{2g},...,x_{n_c-1g}\}$
Collins et al. (1992)	AIM/FI/IMPEC	NM	$\{P, \widetilde{N}_w, \widetilde{N}_1,...,\widetilde{N}_{n_c}\}$
Branco and Rodriguez (1996)	IMPSAT	NM	$\{P, S_w, S_g, x_{1o},...,x_{n_c-2o}\}$
Wang et al. (1997)	FI	NM	$\{P, \widetilde{N}_w, \widetilde{N}_1,...,\widetilde{N}_{n_c}, \ln(K_1),...,\ln(K_{n_c})\}$
Haukas et al. (2007a)	IMPSAT	SOI	$\{P, S_w, S_g, \kappa_1,...,\kappa_{n_c-n_p}\}$
Ayala (2004)	FI	QNM	$\{P, S_w, z_1,...,z_{n_c-1}\}$
This work	FI	NM	$\{P, S_w, z_1,...,z_{n_c-1}\}$

[a] NM – Newton's Method; QNM – Quasi-Newton's Method; MVNM – Minimum Variable Newton Method; OI – One-Iteration; SOI – Sequential with One-Iteration.

the volume error due to the nature of the derivation of the pressure equation. The primary variables for this formulation are pressure and the moles of each component. Watts (1986) presented an IMPSAT (Implicit Pressure and Saturations) approach based on the formulations presented by Acs et al. (1985) and Spillette et al. (1973). The formulation proposed by Watts (1986) was a sequential one-iteration approach where pressure would be solved first and used to calculate a semi-implicit total velocity that could be used to compute saturations. However, as indicated by Quandalle and Savary (1989) the scheme proposed by Watts (1986) have inconsistencies; they proposed a new set of primary variables and flash calculation for solving the inconsistencies and improving the stability of the previous IMPSAT approach. Collins et al. (1992) presented an Adaptive Implicit Method (AIM) that considered pressure and the overall mole concentrations as primary variables that are solved through the material balance equations and a volume constraint. Branco and Rodriguez (1996) modified the formulation proposed by Coats (1980) into an IMPSAT approach by treating the compositions explicitly. Wang et al. (1997) presented a fully implicit, fully coupled approach that solved, in each Newton iteration, all material balance equations and equilibrium constraints. They used pressure, overall mole concentrations, and the logarithm of the equilibrium ratios as primary variables,. Haukas et al. (2007a) proposed a new IMPSAT formulation based on the formulation of Quandalle and Savary (1989) by replacing the phase compositions that were solved explicitly by new variables that were named isochoric variables, which represented the mass changes introduced at constant pressure and volume. This IMPSAT formulation was compared with the IMPSAT implemented in Cao and Aziz (2002) by Haukas et al. (2007b). Ayala (2004) implemented a fully implicit formulation for compositional reservoir simulation using pressure, water saturation, and overall compositions as primary variables; the Jacobian matrix in this work is obtained numerically. The work of Ayala (2004) was used for simulating gas-condensate problems by Ayala et al. (2006). The ideas from the formulation of Ayala (2004) were extended for linear flow in unconventional systems (Zhang and Ayala, 2016) and linear and radial flow (Zhang and Ayala, 2018) using a semi-analytical solution. In these works, the derivatives with respect to the overall composition were also computed numerically. Santos et al. (2013b) implemented several implicit and semi-implicit formulations in GPAS (General Purpose Adaptive Simulator), developed by the University of Texas at Austin, including a new semi-implicit IMPEC formulation based on the ideas presented by Branco and Rodriguez (1996) and Lacroix et al. (2000). Fernandes et al. (2014b) compared the performance of the Acs et al. (1985) and Watts (1986) formulations for Cartesian grids considering three hydrocarbon flash calculation and a total variation diminishing (TVD) originally proposed by Liu et al. (1994). Later, Fernandes et al. (2015b) performed similar study for unstructured grids using the Element based Finite Volume Method (EbFVM) (Baliga and Patankar, 1983; Marcondes and Sepehrnoori, 2010). Fernandes (2014) and Fernandes et al. (2016) presented and implemented a FI version of the formulation proposed by Acs et al. (1985) and compared it to the formulation of Collins et al. (1992). Also, Fernandes et al. (2017) implemented the Coats formulation in UTCOMPRS.

In this work, a new FI approach is proposed, implemented, and tested. The new FI is in part based on formulation uses the FI approach of Collins et al. (1992) as basis. From Collins et al. (1992) approach, a variable set change is performed, allowing the decoupling of one of the equations. Therefore, the final set of primary variables of the new fully implicit approach is based on intensive variables only, and requires the solution of one less equation per gridblock. Additionally, this approach can be easily added to a simulator implemented using pressure and total number of moles as primary variables. The new formulation differs from that of (Ayala, 2004) not only in its solution procedure, but also in the fact that no numerical derivatives are computed, which leads to less number of flash calculation per Newton iteration.

A brief description and classification of some important approaches in the literature along with the one proposed in this work is presented in Table 1. Notice that we emphasize that Ayala (2004) uses a quasi-Newton approach. This is important since the analytical derivatives of the phase compositions with respect to the total composition is a complex procedure. Herein, we took advantage of the analytical derivation with respect to the number of moles of each component, already developed in the literature, and we applied a variable change and elimination procedure to reduce the number of variables to be solved, without loss of derivative accuracy and no extra computation of flash and physical properties.

The new approach is implemented in The University of Texas Compositional Reservoir Simulator (UTCOMPRS). UTCOMPRS is a modified version of the UTCOMP simulator, which initially was developed by Chang (1990), Chang et al. (1990), Perschke (1988), Perschke et al. (1989a), and Perschke et al. (1989b) that considers up to four phase flow (water, oil, gas, and a second oleic phase) with rigorous flash and phase stability calculations. UTCOMP was originally implemented using the Acs et al. (1985) IMPEC approach using Cartesian grids and since the original implementation has been the subject of several improvements and the addition of new capabilities such as unstructured grids (Fernandes et al., 2012; Araújo et al., 2016), corner point (Fernandes et al., 2014a), TVD schemes for unstructured grids

(Fernandes et al., 2013; (Fernandes et al., 2015a), high performance computing (Doroh, 2012), to name few improvements in the UTCOMPRS simulator. The enhanced simulator is referred to as UTCOMPRS.

2. Governing equations

In this work, an isothermal compositional multiphase fluid flow in porous media is considered. The flow equations are obtained by combining the material balance equations with Darcy's law. The mass transfer between phases is assumed to be at local equilibria. A summary of the main assumptions employed in this study is presented below:

1 Isothermal reservoir rock, fluid, and injecting fluids.
2 Local phase equilibrium.
3 Up to three hydrocarbon phases.
4 No hydrocarbon dissolution or solubilization into the aqueous phase.
5 No water mass transfer between the hydrocarbon phases.
6 Phase velocities evaluated through the modified Darcy's law.
7 No water vaporization.

The material balance equations for each hydrocarbon component can then be written as

$$\frac{1}{V_b}\frac{\partial N_k}{\partial t} = \sum_{j=2}^{n_p}\left[\vec{\nabla}\cdot\left(x_{kj}\xi_j\frac{k_{rj}}{\mu_j}\overline{\overline{K}}\cdot(\vec{\nabla}P_j - \rho_j g\vec{\nabla}D)\right) + \vec{\nabla}\cdot(\phi S_j\xi_j\overline{\overline{\Lambda}}_{ij}\cdot\vec{\nabla}x_{ij})\right] - \frac{\dot{q}_k}{V_b}, \quad k = 1, \ldots, n_c, \tag{1}$$

and for water

$$\frac{1}{V_b}\frac{\partial N_w}{\partial t} = \vec{\nabla}\cdot\left(\xi_w\frac{k_{rw}}{\mu_w}\overline{\overline{K}}\cdot(\vec{\nabla}P_w - \rho_w g\vec{\nabla}D)\right) - \frac{\dot{q}_w}{V_b}, \tag{2}$$

where P_j is the pressure of phase j, k_{rj}, ξ_j, and μ_j are the relative permeability, the molar density, and viscosity of j-th phase, respectively. $\overline{\overline{K}}$ is the absolute permeability tensor, V_b is the bulk volume, x_{kj} is the molar fraction of component k in phase j, $\dot{q}_k$ is the source/sink term of component k due to the producing/injecting well, ρ_j is the mass density of phase j, g is the gravity acceleration, D is the depth, S_j is the saturation of phase j, ϕ is the porosity, and $\overline{\overline{\Lambda}}_{ij}$ is the dispersion tensor of component i in phase j. Herein, the subscript w stands for water component or phase, and will be used interchangeably along with the subscripts 1, for aqueous phase, and n_c+1 for the water component. Similarly, subscripts 2 and o stands for oil phase, 3 and g for gas phase, and 4 and l stand for a second oleic phase. In UTCOMPRS, the phase pressures are computed with respect to the oil pressure according to the capillary relationship

$$P_j = P + P_{cjo} \qquad j = 1, \ldots, n_p, \tag{3}$$

where P is the oil pressure (or the next available hydrocarbon phase, in the absence of oil) and P_{cjo} is the capillary pressure of phase j with respect to the reference phase (oil).

The volume constraint is also necessary and is written as

$$\phi = \frac{1}{V_b}\sum_{j=1}^{n_p}\frac{n_j}{\xi_j}, \tag{4}$$

where n_j is the number of moles of phase j.

The porosity is computed as.

$$\phi = \phi^0(1 + C_f(P - P_{ref})), \tag{5}$$

where P_{ref} is a reference pressure, ϕ^o is the reference porosity, and C_f is the rock compressibility.

The dispersion tensor is computed as the sum of the molecular diffusion and the mechanical dispersion as

$$\overline{\overline{\Lambda}}_{ij} = \begin{bmatrix} \Lambda_{xx,ij} & \Lambda_{xy,ij} & \Lambda_{xz,ij} \\ \Lambda_{yx,ij} & \Lambda_{yy,ij} & \Lambda_{yz,ij} \\ \Lambda_{zx,ij} & \Lambda_{zy,ij} & \Lambda_{zz,ij} \end{bmatrix}, \tag{6}$$

where

$$\Lambda_{xx,ij} = \frac{D_{ij}}{\tau} + \frac{\alpha_{\ell j}}{\phi S_j}\frac{u_{xj}^2}{|u_j|} + \frac{\alpha_{tj}}{\phi S_j}\frac{u_{yj}^2}{|u_j|} + \frac{\alpha_{tj}}{\phi S_j}\frac{u_{zj}^2}{|u_j|}, \tag{7}$$

$$\Lambda_{yy,ij} = \frac{D_{ij}}{\tau} + \frac{\alpha_{tj}}{\phi S_j}\frac{u_{xj}^2}{|u_j|} + \frac{\alpha_{\ell j}}{\phi S_j}\frac{u_{yj}^2}{|u_j|} + \frac{\alpha_{tj}}{\phi S_j}\frac{u_{zj}^2}{|u_j|}, \tag{8}$$

$$\Lambda_{zz,ij} = \frac{D_{ij}}{\tau} + \frac{\alpha_{tj}}{\phi S_j}\frac{u_{xj}^2}{|u_j|} + \frac{\alpha_{tj}}{\phi S_j}\frac{u_{yj}^2}{|u_j|} + \frac{\alpha_{\ell j}}{\phi S_j}\frac{u_{zj}^2}{|u_j|}, \tag{9}$$

$$\Lambda_{xy,ij} = \Lambda_{yx,ij} = \frac{(\alpha_{\ell j} - \alpha_{tj})}{\phi S_j}\frac{u_{xj}u_{yj}}{|u_j|}, \tag{10}$$

$$\Lambda_{xz,ij} = \Lambda_{zx,ij} = \frac{(\alpha_{\ell j} - \alpha_{tj})}{\phi S_j}\frac{u_{xj}u_{zj}}{|u_j|}, \tag{11}$$

$$\Lambda_{yz,ij} = \Lambda_{zy,ij} = \frac{(\alpha_{\ell j} - \alpha_{tj})}{\phi S_j}\frac{u_{yj}u_{zj}}{|u_j|}, \tag{12}$$

and

$$|u_j| = \sqrt{u_{xj}^2 + u_{yj}^2 + u_{zj}^2}, \tag{13}$$

where u_{xj}, u_{yj}, and u_{zj} are the Cartesian velocity components of phase j, α_ℓ is the longitudinal dispersivity, α_t is the transversal dispersivity. In UTCOMPRS, the dispersivities may be considered constant or as a function of viscosity according to the model originally developed by Young (1990) for 1D displacement, which was later extended by Ewing et al. (1989) for 2D, and Gharbi (1989). The model was also applied by Krueger (1989) for polymer flooding and Santos et al. (2013a) for miscible gas flooding.

The Peng-Robinson equation of state (EOS) (Peng and Robinson, 1976) is used to compute density and fugacities.

Phase appearance and disappearance is treated using a stability test calculation. Two phase stability test algorithms are implemented in the UTCOMPRS simulator: the stationary point location method (Michelsen, 1982) and the Gibbs free energy minimization algorithm that is similar to the Trangenstein (1987) method and was modified by Perschke (1988) to deal with the equilibrium of three hydrocarbon phases. In general, as commented by Perschke (1988) the stationary method is faster than Gibbs free energy minimization method.

After the phase stability, a flash calculation to evaluate the mole fractions and amount of each hydrocarbon phase is performed. The flash calculation used in UTCOMPRS is a combination of the Accelerated Successive Substitution (ACSS) method (Mehra et al., 1983) with the modified version of the Gibbs free energy minimization method (Perschke, 1988). At the beginning of the flash procedure, the ACSS method is used in order to provide a reasonable initial estimation, and then it is switched to the Gibbs free energy minimization method in order to accelerate the convergence. The switching criteria to change from one method to another is given by (Chang, 1990).

3. Approximate equations

In the new scheme presented in this work, the original approximate equations are equal to the ones of the fully implicit model of Collins et al. (1992). In order to obtain the approximate equations we will use

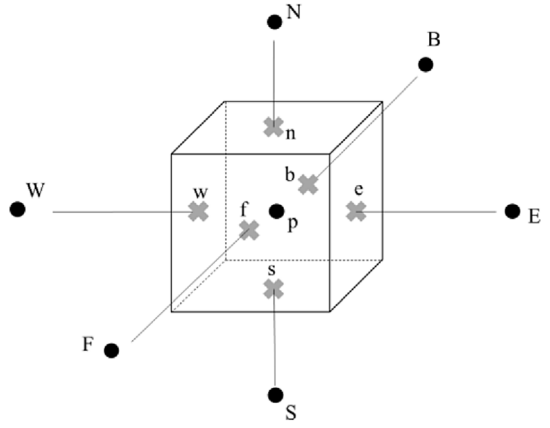

Fig. 1. Illustration of a Cartesian Control-Volume with indexations according to Maliska (2004).

	P_1	$N_{1,1}$	$N_{1,2}$	$N_{1,w}$	P_2	$N_{2,1}$	$N_{2,2}$	$N_{2,w}$	P_3	$N_{3,1}$	$N_{3,2}$	$N_{3,w}$
R_1^P	X	X	X	X								
$R_1^{N_1}$	X	X	X	X	X	X	X	X				
$R_1^{N_2}$	X	X	X	X	X	X	X	X				
$R_1^{N_w}$	X	X	X	X	X	X	X	X				
R_2^P					X	X	X	X				
$R_2^{N_1}$	X	X	X	X	X	X	X	X	X	X	X	X
$R_2^{N_2}$	X	X	X	X	X	X	X	X	X	X	X	X
$R_2^{N_w}$	X	X	X	X	X	X	X	X	X	X	X	X
R_3^P									X	X	X	X
$R_3^{N_1}$					X	X	X	X	X	X	X	X
$R_3^{N_2}$					X	X	X	X	X	X	X	X
$R_3^{N_w}$					X	X	X	X	X	X	X	X

Fig. 2. Illustration of the Jacobian obtained using the Collins et al. formulation a 1D grid with 3 grid-blocks and 2 hydrocarbon components plus water.

	P_1	$Z_{1,1}$	$N_{t,1}$	$S_{w,1}$	P_2	$Z_{1,2}$	$N_{t,2}$	$S_{w,2}$	P_3	$Z_{1,3}$	$N_{t,3}$	$S_{w,3}$
R_1^P	X	X	X	X								
$R_1^{N_1}$	X	X	X	X	X	X		X				
$R_1^{N_2}$	X	X	X	X	X	X		X				
$R_1^{N_w}$	X	X	X	X	X	X		X				
R_2^P					X	X	X	X				
$R_2^{N_1}$	X	X		X	X	X	X	X	X	X		X
$R_2^{N_2}$	X	X		X	X	X	X	X	X	X		X
$R_2^{N_w}$	X	X		X	X	X	X	X	X	X		X
R_3^P									X	X	X	X
$R_3^{N_1}$					X	X		X	X	X	X	X
$R_3^{N_2}$					X	X		X	X	X	X	X
$R_3^{N_w}$					X	X		X	X	X	X	X

Fig. 3. Illustration of the Jacobian obtained using the new formulation for a 1D grid with 3 grid-blocks and 2 hydrocarbon components plus water.

the finite volume method in conjunction with Cartesian grids. Therefore, integrating Eqs. (1) and (2) in time and over a Cartesian control-volume of Fig. 1, using a fully implicit approximation in time and moving all terms of the approximate equation to the same side, the following residual equation is obtained:

$$R_{k,p}^{N} = -(N_{k,p}^{n+1} - N_{k,p}^{n}) + \Delta t \sum_{j=2}^{n_p} [F_{kj,e}^{n+1} - F_{kj,w}^{n+1} + F_{kj,n}^{n+1} - F_{kj,s}^{n+1} + F_{kj,f}^{n+1} - F_{kj,b}^{n+1}] + \Delta t \sum_{j=2}^{n_p} [J_{kj,e}^{n+1} - J_{kj,w}^{n+1} + J_{kj,n}^{n+1} - J_{kj,s}^{n+1} + J_{kj,f}^{n+1} - J_{kj,b}^{n+1}] - \Delta t \dot{q}_{k,p}^{n+1}, \quad k = 1, \ldots, n_c, \tag{14}$$

where $F_{kj,e}$ is the advective mole flux of component k in phase j through the interface east e and $J_{kj,e}$ is the dispersive mole flux of component k in phase j through the interface e. The advective mole fluxes, in each interface, are written as

$$F_{kj,e}^{n+1} = (x_{kj}^{n+1}\xi_j^{n+1}\lambda_j^{n+1})_e T_e [P_E^{n+1} - P_p^{n+1} + P_{cjr,E}^{n+1} - P_{cjr,p}^{n+1} - \rho_{j,e}^{n+1} g(D_E - D_p)], \tag{15}$$

$$F_{kj,w}^{n+1} = (x_{kj}^{n+1}\xi_j^{n+1}\lambda_j^{n+1})_w T_w [P_W^{n+1} - P_p^{n+1} + P_{cjr,W}^{n+1} - P_{cjr,p}^{n+1} - \rho_{j,w}^{n+1} g(D_W - D_p)], \tag{16}$$

$$F_{kj,n}^{n+1} = (x_{kj}^{n+1}\xi_j^{n+1}\lambda_j^{n+1})_n T_n [P_N^{n+1} - P_p^{n+1} + P_{cjr,N}^{n+1} - P_{cjr,p}^{n+1} - \rho_{j,n}^{n+1} g(D_N - D_p)], \tag{17}$$

$$F_{kj,s}^{n+1} = (x_{kj}^{n+1}\xi_j^{n+1}\lambda_j^{n+1})_s T_s [P_S^{n+1} - P_p^{n+1} + P_{cjr,S}^{n+1} - P_{cjr,p}^{n+1} - \rho_{j,s}^{n+1} g(D_S - D_p)], \tag{18}$$

$$F_{kj,f}^{n+1} = (x_{kj}^{n+1}\xi_j^{n+1}\lambda_j^{n+1})_f T_f [P_F^{n+1} - P_p^{n+1} + P_{cjr,F}^{n+1} - P_{cjr,p}^{n+1} - \rho_{j,f}^{n+1} g(D_F - D_p)], \tag{19}$$

$$F_{kj,b}^{n+1} = (x_{kj}^{n+1}\xi_j^{n+1}\lambda_j^{n+1})_b T_b [P_B^{n+1} - P_p^{n+1} + P_{cjr,B}^{n+1} - P_{cjr,p}^{n+1} - \rho_{j,b}^{n+1} g(D_B - D_p)], \tag{20}$$

where T_e is the transmissivity at the interface e.

The dispersive mole fluxes are computed as

$$J_{kj,e}^{n+1} = \Delta Y_p \Delta Z_p \left[2(\phi^{n+1}\xi_j^{n+1}S_j^{n+1}\Lambda_{xx,ij}^{n+1})_e \frac{x_{ij,E}^{n+1} - x_{ij,p}^{n+1}}{\Delta X_p + \Delta X_E} + (\phi^{n+1}\xi_j^{n+1}S_j^{n+1}\Lambda_{xy,ij}^{n+1})_e \frac{x_{ij,Ne}^{n+1} - x_{ij,Se}^{n+1}}{\Delta Y_p + 0.5(\Delta Y_N + \Delta Y_S)} + (\phi^{n+1}\xi_j^{n+1}S_j^{n+1}\Lambda_{xz,ij}^{n+1})_e \frac{x_{ij,Fe}^{n+1} - x_{ij,Be}^{n+1}}{\Delta Z_p + 0.5(\Delta Z_F + \Delta Z_B)} \right], \tag{21}$$

$$J_{kj,w}^{n+1} = \Delta Y_p \Delta Z_p \left[2(\phi^{n+1}\xi_j^{n+1}S_j^{n+1}\Lambda_{xx,ij}^{n+1})_w \frac{x_{ij,W}^{n+1} - x_{ij,p}^{n+1}}{\Delta X_p + \Delta X_W} + (\phi^{n+1}\xi_j^{n+1}S_j^{n+1}\Lambda_{xy,ij}^{n+1})_w \frac{x_{ij,Nw}^{n+1} - x_{ij,Sw}^{n+1}}{\Delta Y_p + 0.5(\Delta Y_N + \Delta Y_S)} + (\phi^{n+1}\xi_j^{n+1}S_j^{n+1}\Lambda_{xz,ij}^{n+1})_w \frac{x_{ij,Fw}^{n+1} - x_{ij,Bw}^{n+1}}{\Delta Z_p + 0.5(\Delta Z_F + \Delta Z_B)} \right], \tag{22}$$

$$J_{kj,n}^{n+1} = \Delta X_p \Delta Z_p \left[2(\phi^{n+1}\xi_j^{n+1}S_j^{n+1}\Lambda_{yy,ij}^{n+1})_n \frac{x_{ij,N}^{n+1} - x_{ij,p}^{n+1}}{\Delta Y_p + \Delta Y_N} + (\phi^{n+1}\xi_j^{n+1}S_j^{n+1}\Lambda_{xy,ij}^{n+1})_n \frac{x_{ij,En}^{n+1} - x_{ij,Wn}^{n+1}}{\Delta X_p + 0.5(\Delta X_E + \Delta X_W)} + (\phi^{n+1}\xi_j^{n+1}S_j^{n+1}\Lambda_{yz,ij}^{n+1})_n \frac{x_{ij,Fn}^{n+1} - x_{ij,Bn}^{n+1}}{\Delta Z_p + 0.5(\Delta Z_F + \Delta Z_B)} \right], \tag{23}$$

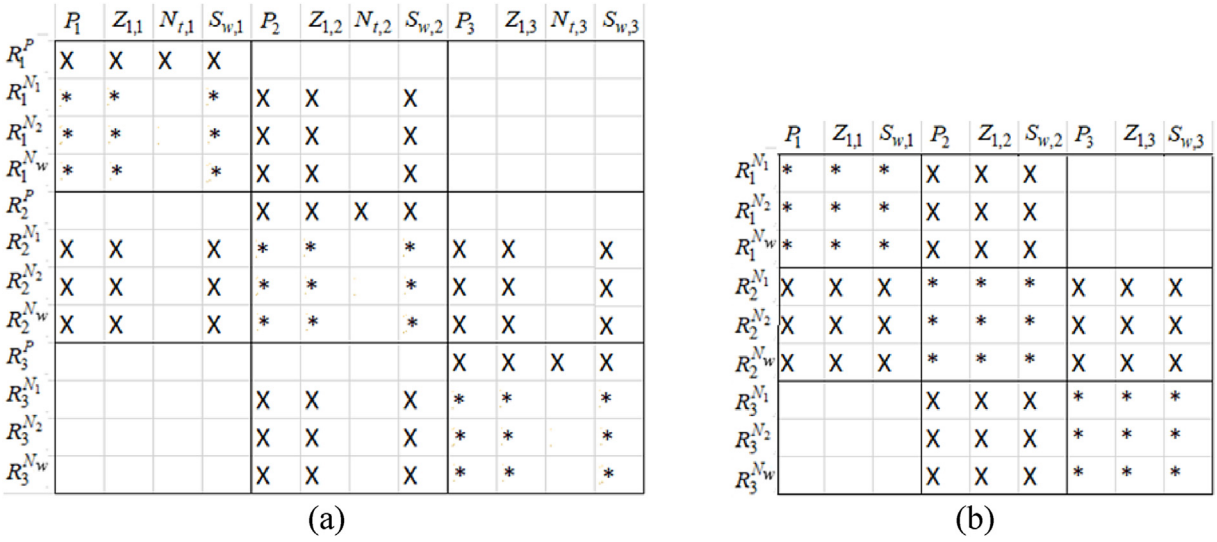

Fig. 4. Illustration of the Jacobian obtained using the new formulation for a 1D grid with 3 grid-blocks and 2 hydrocarbon components plus water. a) After elimination and b) after decoupling the pressure equation.

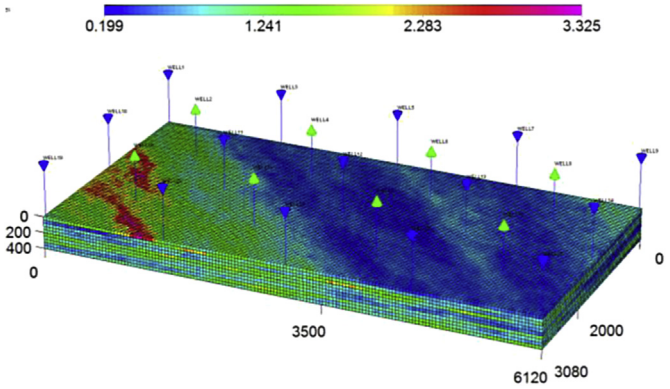

Fig. 5. Absolute permeability field in X and Y directions ($\times 10^{-13}$ m^2) - case study 1.

Table 2
Reservoir data for Case 1.

Property	Value
Length, width, and thickness	1865.37 m, 938.78 m, and 121.92 m
Porosity	0.30
Initial Water Saturation	0.25
Initial Pressure	20.68 MPa
Permeability in z direction	9.87×10^{-15} m^2
Formation Temperature	299.82 K
Gas Injection Rate	4.92 m^3/s (internal wells), 2.46 m^3/s (lateral wells), 1.23 m^3/s (corner wells)
Producer's Bottom Hole Pressure	20.68 MPa
Reservoir's initial composition (CO_2, C_1, and nC_{16})	0.01, 0.19, and 0.80
Injection fluid composition (CO_2, C_1, and nC_{16})	0.95, 0.05 and 0.00

Table 3
Relative permeability data for Case 1.

Property	Value
Model	Stone II
End point relative permeabilities (k_{rw}, k_{ro}, k_{rg})	1.0, 1.0, and 1.0
Exponents (e_w, e_{ow}, e_{og}, e_g)	1.0, 1.0, 1.0, and 1.0
Residual saturations (S_{wr}, S_{owr}, S_{ogr}, S_{gr})	0.25, 0.0, 0.0, and 0.0

Table 4
Pseudo-component data for Case 1.

Component	P_c (Mpa)	T_c (K)	Vc (m^3/mol)	M_w (g/mol)	Ω
CO_2	7.388	304.206	9.395×10^{-5}	44.010	0.2250
C_1	4.600	190.600	9.988×10^{-5}	16.043	0.0225
nC_{10}	1.738	734.684	8.170×10^{-4}	222.000	0.6837
Binary Interaction Coefficients					
CO_2/C_1		0.1			
CO_2/nC_{10}		0.125			

$$J_{kj,s}^{n+1} = \Delta X_p \Delta Z_p \left[2(\phi^{n+1}\xi_j^{n+1} S_j^{n+1} \Lambda_{yy,ij}^{n+1})_s \frac{x_{ij,S}^{n+1} - x_{ij,p}^{n+1}}{\Delta Y_p + \Delta Y_S} + (\phi^{n+1}\xi_j^{n+1} S_j^{n+1} \Lambda_{xy,ij}^{n+1})_s \frac{x_{ij,Es}^{n+1} - x_{ij,Ws}^{n+1}}{\Delta X_p + 0.5(\Delta X_E + \Delta X_W)} + (\phi^{n+1}\xi_j^{n+1} S_j^{n+1} \Lambda_{yz,ij}^{n+1})_s \frac{x_{ij,Fs}^{n+1} - x_{ij,Bs}^{n+1}}{\Delta Z_p + 0.5(\Delta Z_F + \Delta Z_B)} \right], \quad (24)$$

$$J_{kj,f}^{n+1} = \Delta X_p \Delta Y_p \left[2(\phi^{n+1}\xi_j^{n+1} S_j^{n+1} \Lambda_{zz,ij}^{n+1})_f \frac{x_{ij,F}^{n+1} - x_{ij,p}^{n+1}}{\Delta Z_p + \Delta Z_F} + (\phi^{n+1}\xi_j^{n+1} S_j^{n+1} \Lambda_{xz,ij}^{n+1})_f \frac{x_{ij,Ef}^{n+1} - x_{ij,Wf}^{n+1}}{\Delta X_p + 0.5(\Delta X_E + \Delta X_W)} + (\phi^{n+1}\xi_j^{n+1} S_j^{n+1} \Lambda_{yz,ij}^{n+1})_f \frac{x_{ij,Nf}^{n+1} - x_{ij,Sf}^{n+1}}{\Delta Y_p + 0.5(\Delta Y_N + \Delta Y_S)} \right], \quad (25)$$

$$J_{kj,b}^{n+1} = \Delta X_p \Delta Y_p \left[2(\phi^{n+1}\xi_j^{n+1} S_j^{n+1} \Lambda_{zz,ij}^{n+1})_b \frac{x_{ij,B}^{n+1} - x_{ij,p}^{n+1}}{\Delta Z_p + \Delta Z_B} + (\phi^{n+1}\xi_j^{n+1} S_j^{n+1} \Lambda_{xz,ij}^{n+1})_b \frac{x_{ij,Eb}^{n+1} - x_{ij,Wb}^{n+1}}{\Delta X_p + 0.5(\Delta X_E + \Delta X_W)} + (\phi^{n+1}\xi_j^{n+1} S_j^{n+1} \Lambda_{yz,ij}^{n+1})_b \frac{x_{ij,Nb}^{n+1} - x_{ij,Sb}^{n+1}}{\Delta Y_p + 0.5(\Delta Y_N + \Delta Y_S)} \right], \quad (26)$$

The volume constraint equation in its residual form is written, for each gridblock, as

$$R_p^P = \sum_{j=1}^{n_p} \frac{n_{j,p}^{n+1}}{\xi_{j,p}^{n+1}} - V_{b,p}\phi_p^{n+1}. \quad (27)$$

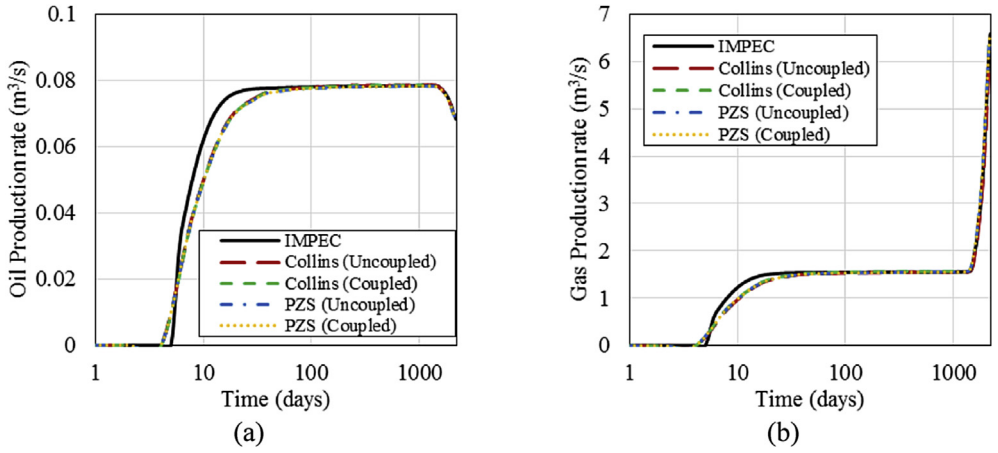

Fig. 6. Production rates for case study 1. a) Oil and b) gas.

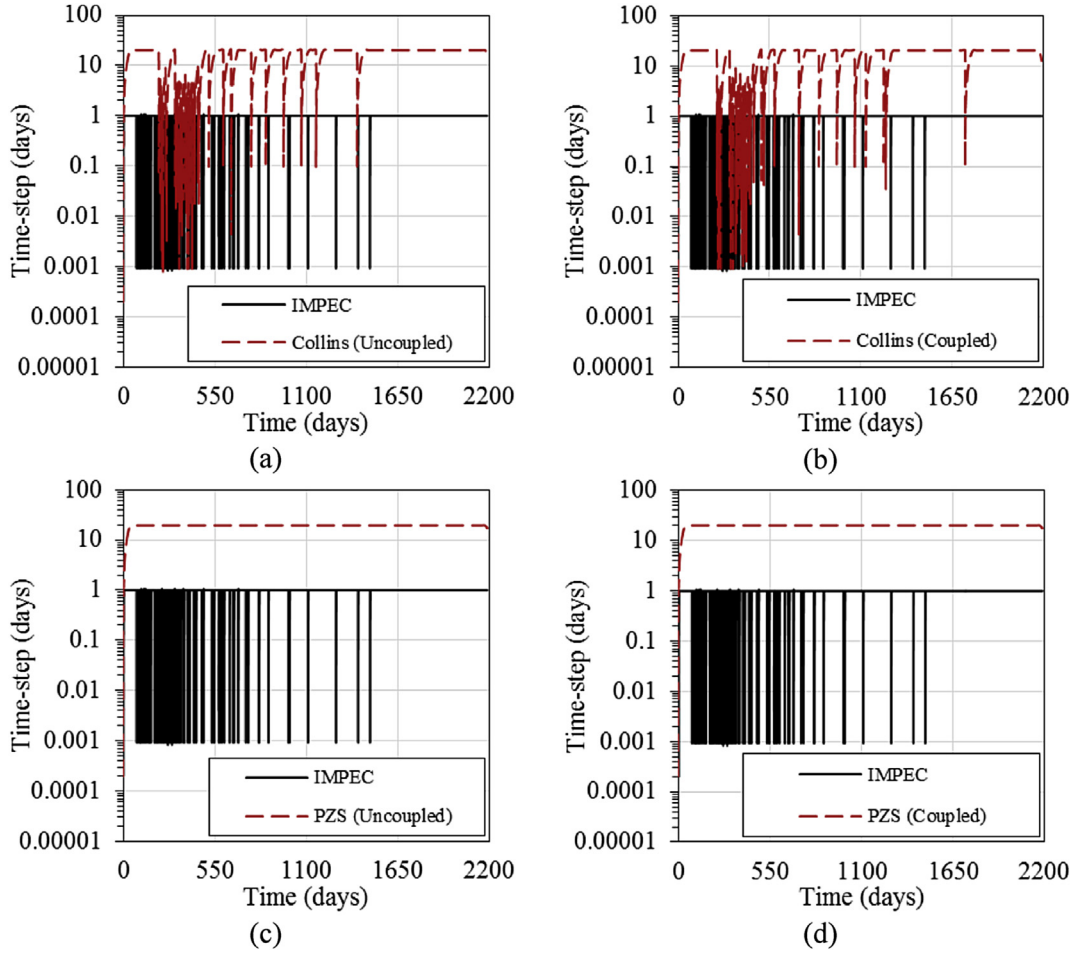

Fig. 7. Time-step profile comparison against IMPEC - case study 1. a) Collins (uncoupled), b) Collins (coupled), c) PZS (uncoupled) and d) PZS (coupled).

4. Well model

In UTCOMPRS, wells can be controlled by either total constant flow rate or constant bottom hole pressure. For the scope of this work, injector wells are controlled by total constant flow rate and producer wells are controlled by constant bottom hole.

Injector wells controlled by constant total flow rate have the mole rate computed at each gridblock it intercepts as

$$\dot{q}_{k,r}^{n+1} = \dot{q}_{Tk} \frac{WI_r \sum_{j=1}^{n_p} \lambda_{j,r}^{n+1}}{\sum_{v=1}^{n_{seg}} \left[WI_v \sum_{j=1}^{n_p} \lambda_{j,v}^{n+1} \right]}, \tag{28}$$

where n_{seg} is the number of segments of the well, q_{Tk} is the total mole rate of component k, q_{kr} is the mole rate of component k in segment r. and WI_r is the productivity index of the r-th segment of the well, which is computed assuming Peaceman's model (Peaceman, 1978, 1983).

The mole rate for constant bottom hole pressure producer wells are

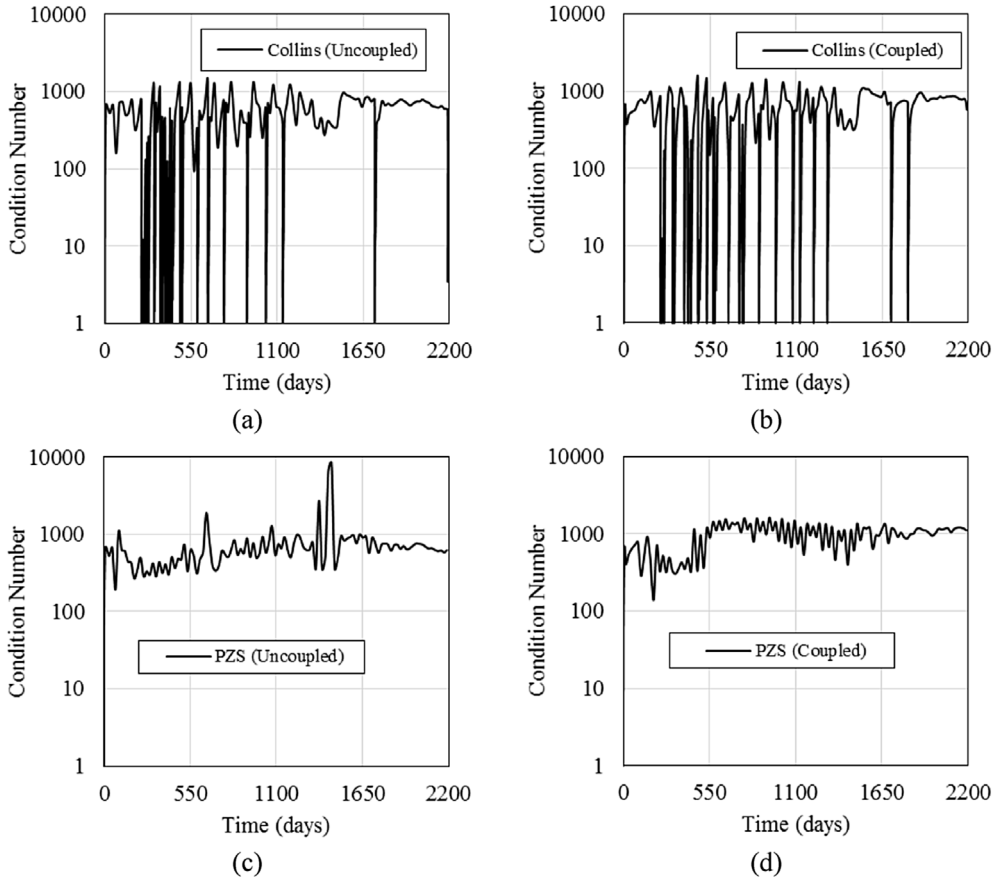

Fig. 8. Maximum condition number per time-step profile comparison against IMPEC - case study 1. a) Collins (uncoupled), b) Collins (coupled), c) PZS (uncoupled) and d) PZS (coupled).

computed as

$$\dot{q}_{k,r}^{n+1} = \sum_{j=1}^{n_p} x_{kj,r}^{n+1} \xi_{kj,r}^{n+1} WI_r (P_r^{n+1} + P_{cjo,r}^{n+1} - P_{wf,r}^{n+1}), \tag{29}$$

where $P_{wf,r}^{n+1}$ is the well pressure of segment r and P_r^{n+1} is the pressure of the gridblock at which the well segment r is intercepted.

5. The new algorithm

It is important to present a brief description of intensive and extensive variables as defined in thermodynamics. An extensive variable depends of the amount of mass or size of the system as opposed to intensive variables. Examples of extensive variables are volume, mass, and enthalpy, while mole fractions, density, and specific enthalpy are examples of intensive variables.

The main idea of the formulation proposed here is to change the set of variables considered by Collins et al. (1992), which was based on extensive variables to a set of only intensive variables. This is advantageous because we need to solve one less unknown per gridblock to determine the intensive state. The amount of moles/mass in the system can then be determined with the intensive variables using the equation that is eliminated from the linear system. Herein, the set of primary variables are first changed from pressure and number of moles $\{P, N_k\}$ to pressure, overall hydrocarbon composition, total hydrocarbon moles, and water saturation $\{P, Z_i, N_t, S_w\}$. The total hydrocarbon moles is then decoupled from the system in order to reduce one unknown $\{P, Z_i, S_w\}$. Therefore, the number of primary variables is reduced from n_c+2 to n_c+1. First in this algorithm, the Newton Raphson method is used considering the primary variables proposed by Collins et al. (1992),

$$\overline{J}_k^{n+1} \Delta\vec{x}_k^{n+1} = -\vec{r}_k^{n+1}, \tag{30}$$

where $\Delta\vec{x}_k^{n+1}$ are the changes in the primary variables at iteration k, $\vec{r}_k^{n+1}$ are the residues of the volume balance and material balances at iteration k, and $\overline{J}_k^{n+1}$ is the Jacobian matrix at iteration k. For better illustration, Eq. (30) is written for a 1D grid using a blocked Jacobian, blocked unknowns vector, and blocked residues vector below:

$$\begin{bmatrix} J_{1,P} & J_{1,E} & & & & \\ J_{2,W} & J_{2,P} & J_{2,E} & & & \\ & \ddots & \ddots & \ddots & & \\ & & J_{N_B-1,W} & J_{N_B-1,P} & J_{N_B-1,E} & \\ & & & J_{N_B,W} & J_{N_B,P} & \end{bmatrix} \begin{bmatrix} \Delta X_1 \\ \Delta X_2 \\ \vdots \\ \Delta X_{N_B-1} \\ \Delta X_{N_B} \end{bmatrix} = - \begin{bmatrix} R_1 \\ R_2 \\ \vdots \\ R_{N_B-1} \\ R_{N_B} \end{bmatrix}, \tag{31}$$

where, using Collins et al. (1992) formulation we have

$$J_{i,j} = \begin{bmatrix} \frac{\partial R_i^P}{\partial P_j} & \frac{\partial R_i^P}{\partial N_{1,j}} & \cdots & \frac{\partial R_i^P}{\partial N_{nc,j}} & \frac{\partial R_i^P}{\partial N_{nc+1,j}} \\ \frac{\partial R_i^{N1}}{\partial P_j} & \frac{\partial R_i^{N1}}{\partial N_{1,j}} & \cdots & \frac{\partial R_i^{N1}}{\partial N_{nc,j}} & \frac{\partial R_i^{N1}}{\partial N_{nc+1,j}} \\ \vdots & \vdots & \ddots & \vdots & \vdots \\ \frac{\partial R_i^{Nnc}}{\partial P_j} & \frac{\partial R_i^{Nnc}}{\partial N_{1,j}} & \cdots & \frac{\partial R_i^{Nnc}}{\partial N_{nc,j}} & \frac{\partial R_i^{Nnc}}{\partial N_{nc+1,j}} \\ \frac{\partial R_i^{Nnc+1}}{\partial P_j} & \frac{\partial R_i^{Nnc+1}}{\partial N_{1,j}} & \cdots & \frac{\partial R_i^{Nnc+1}}{\partial N_{nc,j}} & \frac{\partial R_i^{Nnc+1}}{\partial N_{nc+1,j}} \end{bmatrix}, \tag{32}$$

$$\Delta X_i = \begin{bmatrix} \Delta P_i \\ \Delta N_{i,1} \\ \vdots \\ \Delta N_{i,n_c} \\ \Delta N_{i,n_c+1} \end{bmatrix}, \tag{33}$$

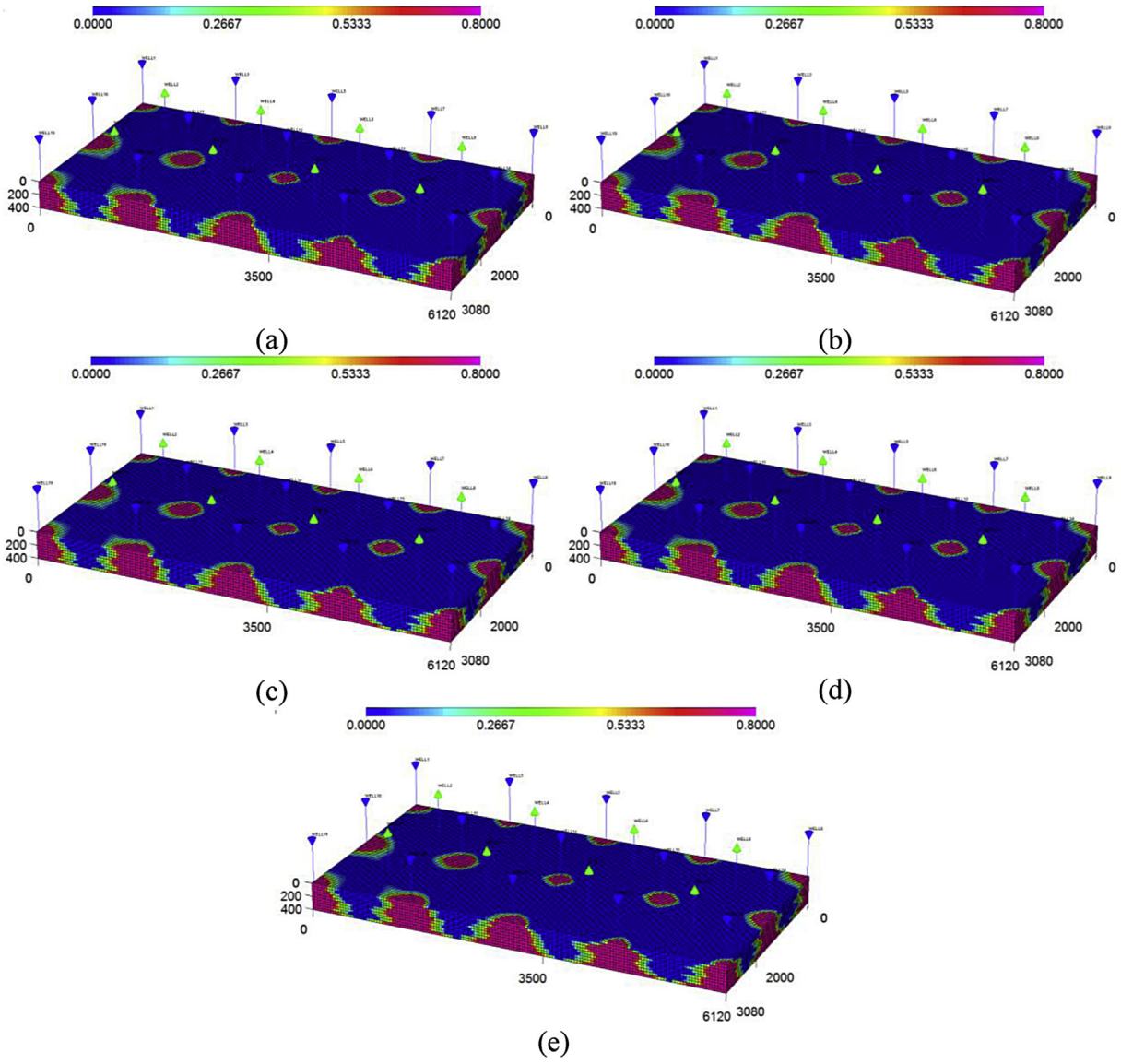

Fig. 9. Gas saturation field - case study 1 at 2190 days. a) Collins et al. with uncoupled wells; b) Collins et al. with wells coupled; c) PZS with wells uncoupled; d) PZS with wells coupled; and e) IMPEC.

Table 5
CPU Time and number of Newton iterations for Case 1.

Formulation	CPU Time (s)	Normalized CPU Time	Total number of Newton iterations	Average Highest Condition Number	Total Number of Solver Iterations
IMPEC	3640	1.00	–	–	–
Collins et al. with uncoupled wells	4007	1.11	646	577	8194
Collins et al. with coupled wells	3758	1.03	632	631	8663
PZS with uncoupled wells	2060	0.56	383	779	8662
PZS with coupled wells	2673	0.73	371	958	10,746

and

$$R_i = \begin{bmatrix} R_i^P \\ R_i^{N_1} \\ \vdots \\ R_i^{N_{nc}} \\ R_i^{N_{nc+1}} \end{bmatrix}. \quad (34)$$

The Jacobian for Collins et al. (1992) formulation considering a 1D discretization with 2 hydrocarbon components plus water is shown in Fig. 2. From the figure, it can be observed that the first equation depends only of the variables of the gridblock itself.

The Jacobian of Eq. (30) and Fig. 2 is changed to the new variable set by changing the derivatives, which are given by the following expressions:

Table 6
Pseudo-component data - case study 2 (Killough and Kossack, 1987).

Component	P_c (MPa)	T_c (K)	Vc (m^3/mol)	M_w (g/mol)	ω
C_1	4.60	190.56	9.98×10^{-5}	16.00	0.0130
C_3	4.25	369.83	2.00×10^{-4}	44.10	0.1520
C_6	3.01	507.45	3.70×10^{-4}	86.20	0.3010
C_{10}	2.10	617.67	6.30×10^{-4}	142.30	0.4880
C_{15}	1.38	705.56	1.04×10^{-3}	206.00	0.6500
C_{20}	1.12	766.67	1.34×10^{-3}	282.00	0.8500
Binary Interaction Coefficients					
C_1/C_{15}		0.05			
C_1/C_{20}		0.05			
C_3/C_{15}		0.005			
C_3/C_{20}		0.005			

$$\left(\frac{\partial R^P}{\partial P}\right)_{z,N_t,S_w} = \left(\frac{\partial R^P}{\partial P}\right)_{N_k,N_w} + \left(\frac{\partial R^P}{\partial N_w}\right)_{P,N_k} [S_w V_b \phi^0 \xi_w^0 \{C_f(1 + C_w(P - P_{ref})) + C_w(1 + C_f(P - P_{ref}))\}], \quad (35)$$

$$\left(\frac{\partial R^P}{\partial Z_i}\right)_{P,Z_k \neq Z_i,N_t,S_w} = N_t \left(\left(\frac{\partial R^P}{\partial N_i}\right)_{P,N_k \neq N_i,N_w} - \left(\frac{\partial R^P}{\partial N_{n_c}}\right)_{P,N_k \neq N_{n_c},N_w}\right), \quad i = 1, \ldots, n_c - 1, \quad (36)$$

Table 7
Reservoir data - case study 2.

Property	Value
Length, width, and thickness	170.688 m, 170.688 m, and 30.48 m
Porosity	0.35
Initial Water Saturation	0.30
Initial Pressure	10.34 MPa
Formation Temperature	344.26 K
Longitudinal Dispersivity	4.74 m
Transverse Dispersivity	0.47 m
Longitudinal parameter for Young's Dispersion	0.91
Transverse parameter for Young's Dispersion	0.91
Gas Injection Rate	0.328 m^3/s
Producer's Bottom Hole Pressure	8.96 MPa
Reservoir's initial composition (C_1, C_3, C_6, C_{10}, C_{15}, and C_{20})	0.50, 0.03, 0.07, 0.20, 0.15, and 0.05
Injection fluid composition (C_1, C_3, C_6, C_{10}, C_{15}, and C_{20})	0.77, 0.20, 0.01, 0.01, 0.005 and 0.005

Table 8
Relative permeability data - case study 2.

Property	Value
Model	Stone II
End point relative permeabilities (k_{rw}, k_{ro}, k_{rg})	0.4, 0.9, and 0.9
Exponents (e_w, e_{ow}, e_{og}, e_g)	3.0, 2.0, 2.0, and 3.0
Residual saturations (S_{wr}, S_{owr}, S_{ogr}, S_{gr})	0.3, 0.1, 0.1, and 0.0

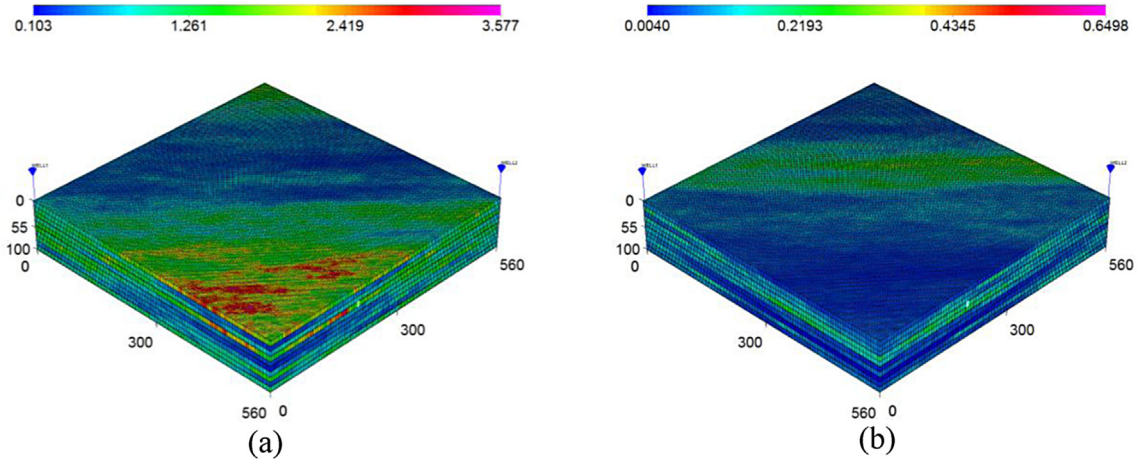

Fig. 10. Permeability distribution ($\times 10^{-13}$ m^2) - case study 2. a) X and Y directions and b) Z directions.

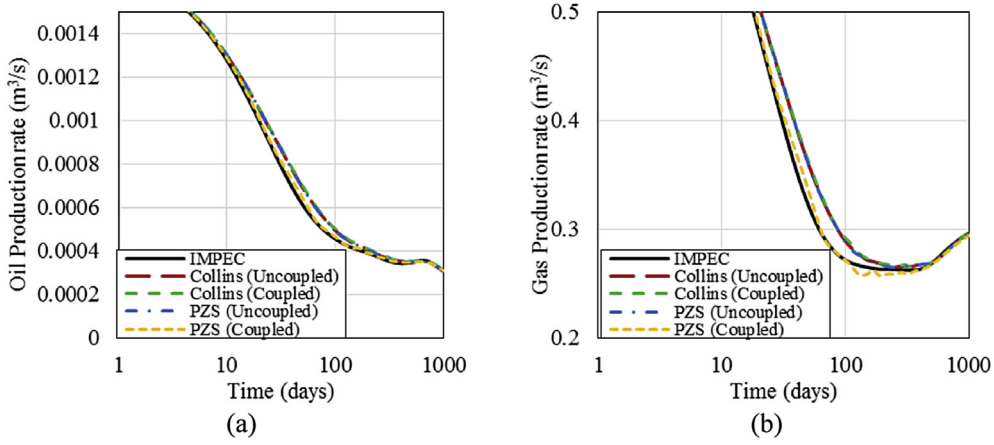

Fig. 11. Production rates for case study 2. a) Oil and b) gas.

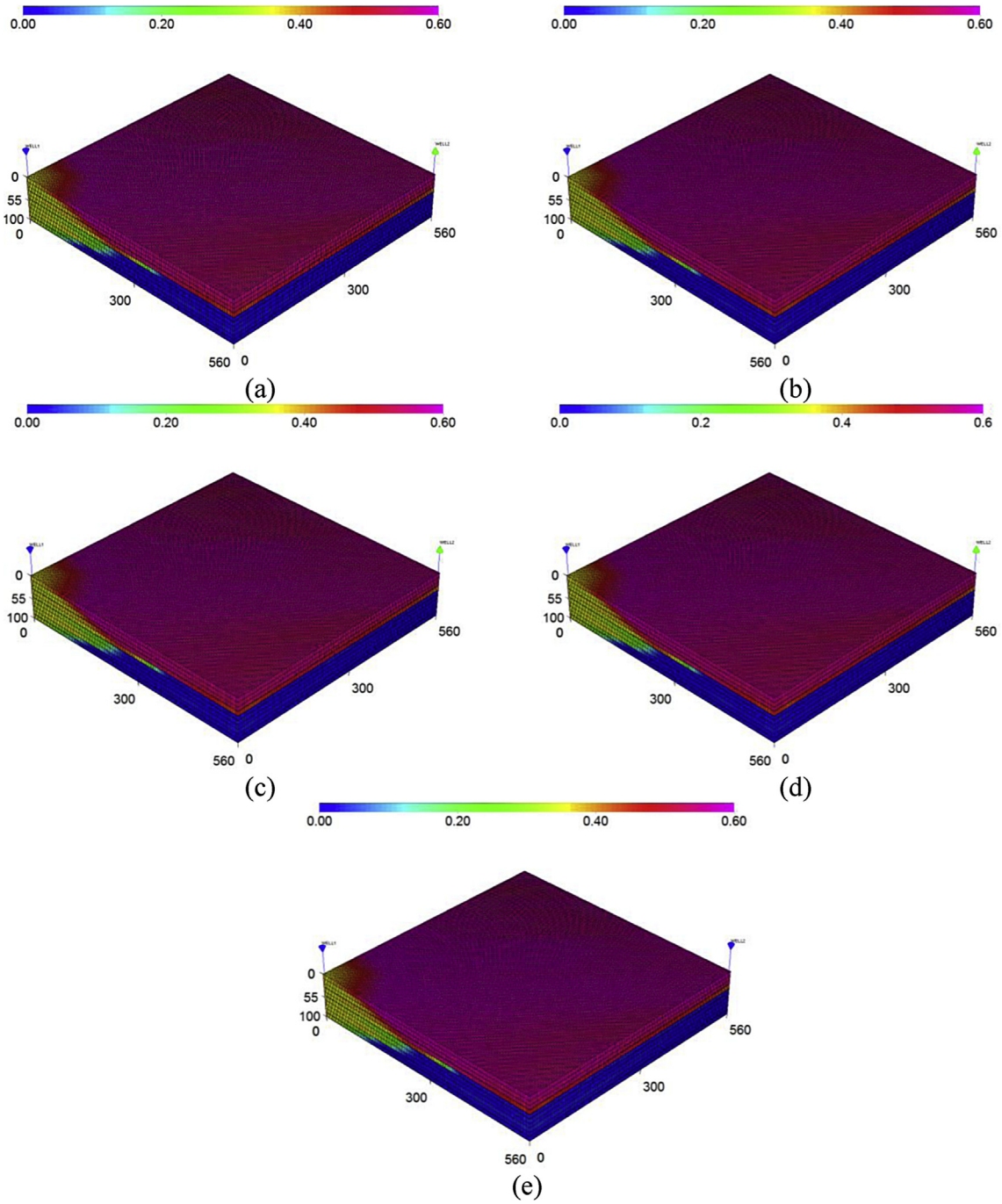

Fig. 12. Gas saturation field - case study 2 at 1000 days. a) Collins et al. with wells uncoupled; b) Collins et al. with wells coupled; c) PZS with wells uncoupled; d) PZS with wells coupled; and e) IMPEC.

$$\left(\frac{\partial R^P}{\partial N_t}\right)_{P,Z_k,S_w} = \sum_{k=1}^{n_c-1} Z_k \left(\left(\frac{\partial R^P}{\partial N_k}\right)_{P,N_k \neq N_i,N_w} - \left(\frac{\partial R^P}{\partial N_{n_c}}\right)_{P,N_{nc} \neq N_i,N_w} \right), \tag{37}$$

$$\left(\frac{\partial R^P}{\partial S_w}\right)_{P,Z_k,N_t} = \left(\frac{\partial R^P}{\partial N_w}\right)_{P,N_k} V_b \phi^0 \xi_w^0 [1 + C_f(P - P_{ref})][1 + C_w(P - P_{ref})], \tag{38}$$

$$\left(\frac{\partial R_j^N}{\partial P}\right)_{z,N_t,S_w} = \left(\frac{\partial R_j^N}{\partial P}\right)_{N_k,N_w} + \left(\frac{\partial R_j^N}{\partial N_w}\right)_{P,N_k} [S_w V_b \phi^0 \xi_w^0 \{C_f(1 + C_w(P - P_{ref})) + C_w(1 + C_f(P - P_{ref}))\}], j = 1, \ldots, n_c + 1, \tag{39}$$

$$\left(\frac{\partial R_j^N}{\partial Z_i}\right)_{P,Z_k \neq Z_i,N_t,S_w} = N_t \left(\left(\frac{\partial R_j^N}{\partial N_i}\right)_{P,N_k \neq N_i,N_w} - \left(\frac{\partial R_j^N}{\partial N_{n_c}}\right)_{P,N_k \neq N_{n_c},N_w} \right), i = 1, \ldots, n_c - 1; \; j = 1, \ldots, n_c + 1, \tag{40}$$

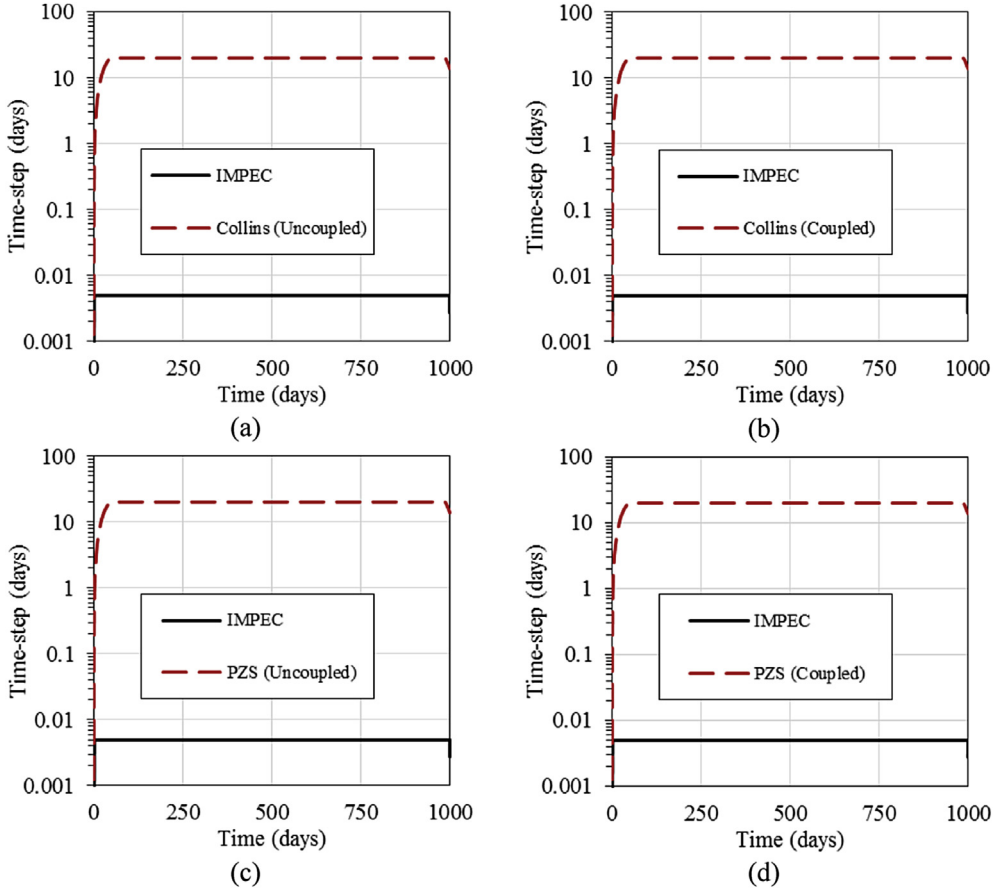

Fig. 13. Time-step profile comparison against IMPEC - case study 2. a) Collins (uncoupled), b) Collins (coupled), c) PZS (uncoupled) and d) PZS (coupled).

$$\left(\frac{\partial R_j^N}{\partial N_t}\right)_{P,Z_k,S_w} = \sum_{k=1}^{n_c-1} Z_k \left(\left(\frac{\partial R_j^N}{\partial N_k}\right)_{P,N_k \neq N_i,N_w} - \left(\frac{\partial R_j^N}{\partial N_{n_c}}\right)_{P,N_{nc} \neq N_i,N_w} \right), \; j = 1, \ldots, n_c + 1, \tag{41}$$

$$\left(\frac{\partial R_j^N}{\partial S_w}\right)_{P,Z_k,N_t} = \left(\frac{\partial R_j^N}{\partial N_w}\right)_{P,N_k} V_b \phi^0 \xi_w^0 [1 + C_f (P - P_{ref})][1 + C_w (P - P_{ref})], j = 1, \ldots, n_c + 1. \tag{42}$$

Despite of the variable change, one might notice that in the new variable set only N_t is an extensive variable. This is important, since the flux terms (Eq. (15) through (26)) are function of intensive variables only. Therefore, the derivatives of flux term with respect to the total number of moles is zero in the off-diagonal gridblocks.

The Jacobian illustrated in Fig. 2, after applying Eq. (35) through (42), is now illustrated in Fig. 3. From Fig. 3, it can be observed that the pressure equation can be used to eliminate the dependence with the total number of moles from the individual material balance equations. This elimination leads to the new Jacobian shown in Fsig. 4a. From the Jacobian in Fig. 4a, it is possible to obtain pressure and the overall compositions without the need of the pressure equation (first line of each block). The Jacobian used by the new system of equations is then illustrated in Fig. 4b, where it can be observed that one less equation is solved per grid-block. After solving the linear system for pressure, overall composition, and water saturation the total number of moles is obtained by inserting these variables in the first equation that was removed from the Jacobian presented in Fig. 4a.

Additionally, the wells can be considered coupled or decoupled. In the decoupled approach, a gridblock is assumed to consider only the segment that intercepts itself in the calculation of the Jacobian. The contribution of the other segments are transferred to the residues. On the other hand, in the coupled approach, it is considered extra equations for each component in each segment, similar to the approach presented by Cao (2002). Such approach is beneficial when a well intercepts several gridblocks because it improves the convergence of the method. Both cases are considered in this work, and the results concerning these two approaches will be presented in the next section.

As it may be noted, the derivatives of properties such as viscosity and density with respect to the primary variables are not simple to be obtained, once these properties are function of the phase composition. Therefore, the derivatives of phase composition with respect to the primary variables must be obtained. The procedure to obtain these derivatives is presented in Appendix A. Since we only perform the variable change after the Jacobian for the P and N (Pressure and number of moles) is already obtained, we just need to obtain these derivatives with respect to pressure and the total number of moles as in the original P and N approach.

6. Results and discussion

For all cases presented in this section, the linear systems were solved by the GMRES method (Saad and Schultz, 1986) with restart option and the ILU preconditioner using the PETSc package (Balay et al., 2013). The post-processing of the fields' properties (saturations, compositions, permeability, etc) was performed using the S3Graf package from ScienceSoft.

Three case studies are presented for testing and validating of the new fully implicit formulation proposed in this work. The first case study considers a CO_2 injection in a high pressure heterogeneous reservoir. The second case study considers a gas flooding in a heterogeneous reservoir with a gas cap. Finally, the last case study simulates a

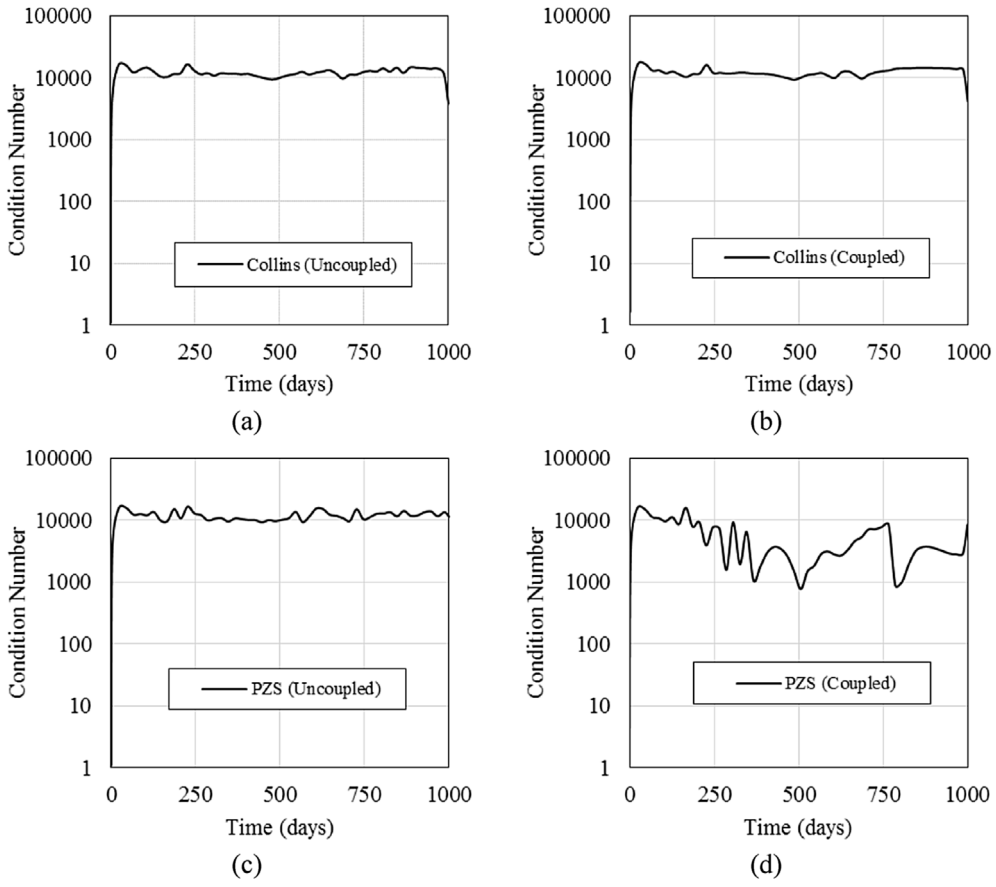

Fig. 14. Maximum condition number per time-step profile comparison against IMPEC - case study 2. a) Collins (uncoupled), b) Collins (coupled), c) PZS (uncoupled) and d) PZS (coupled).

Table 9
CPU Time and number of Newton iterations – case study 2.

Formulation	CPU Time (s)	Normalized CPU Time	Total number of Newton iterations	Average Highest Condition Number	Total Number of Solver Iterations
IMPEC	673,463	1.00	–	–	–
Collins et al. with uncoupled wells	27,016	0.040	229	12,145	12,929
Collins et al. with coupled wells	24,540	0.036	218	12,237	12,324
PZS with uncoupled wells	24,337	0.036	263	11,960	14,902
PZS with coupled wells	22,562	0.033	242	5375	13,635

Table 10
Pseudo-component data - case study 3 (Khan et al., 1992).

Component	P_c (MPa)	T_c (K)	Vc (m^3/mol)	M_w (g/mol)	Ω
CO_2	7.38	304.20	9.40×10^{-5}	44.01	0.225
C_1	4.60	190.60	9.90×10^{-5}	16.04	0.008
$C_{2\text{-}3}$	4.50	344.21	1.81×10^{-4}	37.20	0.131
$C_{4\text{-}6}$	3.40	463.22	3.07×10^{-4}	69.50	0.240
$C_{7\text{-}15}$	2.17	605.75	5.99×10^{-4}	140.96	0.618
$C_{16\text{-}27}$	1.65	751.02	1.13×10^{-3}	280.99	0.957
C_{28+}	1.64	942.48	2.09×10^{-3}	519.62	1.268
Binary Interaction Coefficients					
CO_2/C_1		0.055			
$CO_2/C_{2\text{-}3}$		0.055			
$CO_2/C_{4\text{-}6}$		0.055			
$CO_2/C_{7\text{-}15}$		0.105			
$CO_2/C_{16\text{-}27}$		0.105			
CO_2/C_{28+}		0.105			

Table 11
Reservoir data - case study 3.

Property	Value
Length, width, and thickness	1219.2 m, 1219.2 m, and 60.96 m
Initial Water Saturation	0.25
Initial Pressure	7.58 MPa
Formation Temperature	313.706 K
Longitudinal Dispersivity	4.74 m
Transverse Dispersivity	0.47 m
Longitudinal parameter for Young's Dispersion	9.1
Transverse parameter for Young's Dispersion	9.1
Injector's Bottom Hole Pressure	8.62 MPa (all injectors)
Producer's Bottom Hole Pressure	7.58 MPa (all producers)
Reservoir's initial composition (CO_2, C_1, $C_{2\text{-}3}$, $C_{4\text{-}6}$, $C_{7\text{-}15}$, $C_{16\text{-}27}$, and C_{28+})	0.0337, 0.0861, 0.1503, 0.1671, 0.3304, 0.1611, and 0.0713
Injection fluid composition (CO_2 and C_1)	0.95, 0.05

Table 12
Relative permeability data - case study 3.

Property	Value
Model	Corey
End point relative permeabilities (k_{rw}, k_{ro}, k_{rg}, k_{r2l})	0.21, 0.7, 0.35, and 0.35
Exponents (e_w, e_{ow}, e_{og}, e_g, e_{2lw}, e_{2lg})	1.5, 2.5, 2.5, 2.5, 2.5, and 2.5
Residual saturations (S_{wr}, S_{owr}, S_{ogr}, S_{gr}, S_{2lr}, S_{2lr})	0.25, 0.2, 0.2, 0.05, 0.2 and 0.2

CO_2 injection in a heterogeneous reservoir with inactive cells and a three-phase hydrocarbon flash calculation. The results will be compared in terms of the production rates, time-step profile, property fields, CPU times, and Newton iterations. The new PZS formulation implemented in this work is tested for both coupled and uncoupled wells and is compared to the formulations of Acs et al. (1985) and Collins et al. (1992).

In the first case study a reservoir with heterogeneity in the X and Y permeabilities is considered. Twenty-three wells are considered in a 153 × 77 × 10 grid. The permeability field is presented in Fig. 5.

The reservoir data is presented in Table 2. The relative permeability model used for this case was the Stone II (Stone, 1973). Data for the relative permeabilities used in this case are presented in Table 3. Additionally, no dispersion was considered for this case study. The simulation is run for up to 2190 days (about 0.22 PVI). The properties for each component are given in Table 4.

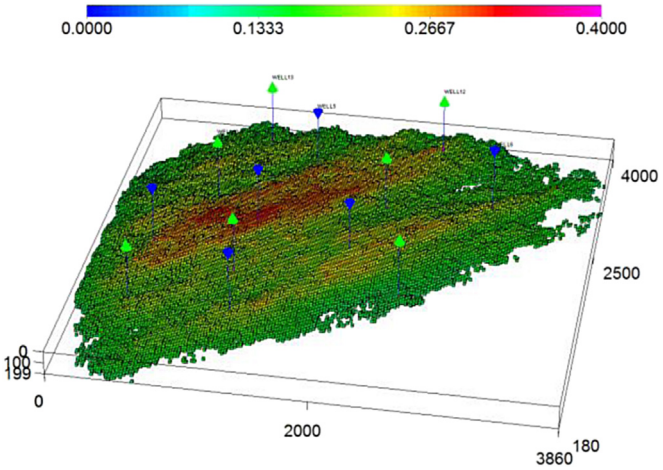

Fig. 17. Reservoir porosity - case study 3.

A comparison of the oil and gas production rates is presented in Fig. 6 in semi-log plots, where it can be observed a good agreement of the production curves obtained with all the formulations. The choice for semi-log plot was taken here since there could be observed no difference in the normal plot. Differences between the IMPEC and the FI approaches can be observed in the early stages of production, which are caused by the larger difference in time-step size. However, any difference between the FI approaches cannot be observed.

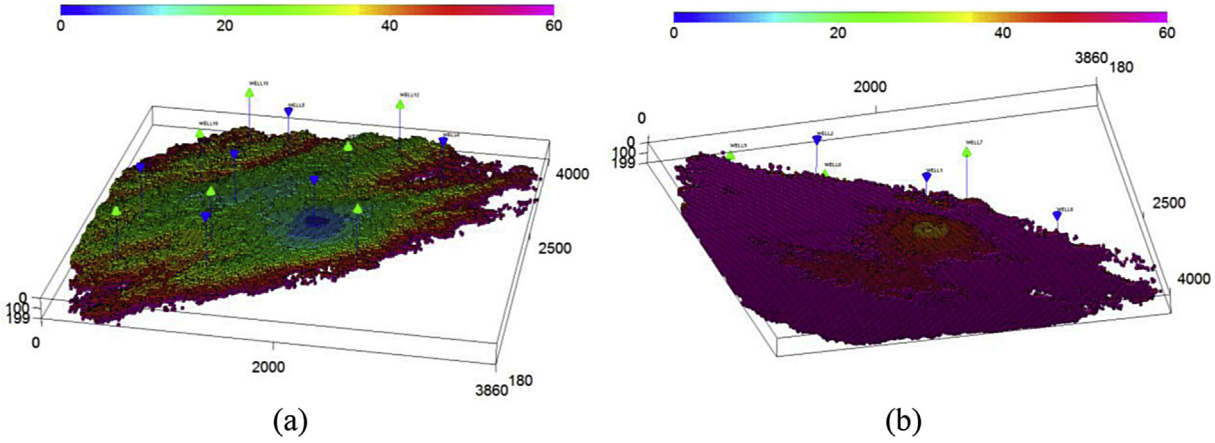

Fig. 15. Reservoir depth (m) from the top and bottom of the reservoir - case study 3. a) top view and b) bottom view.

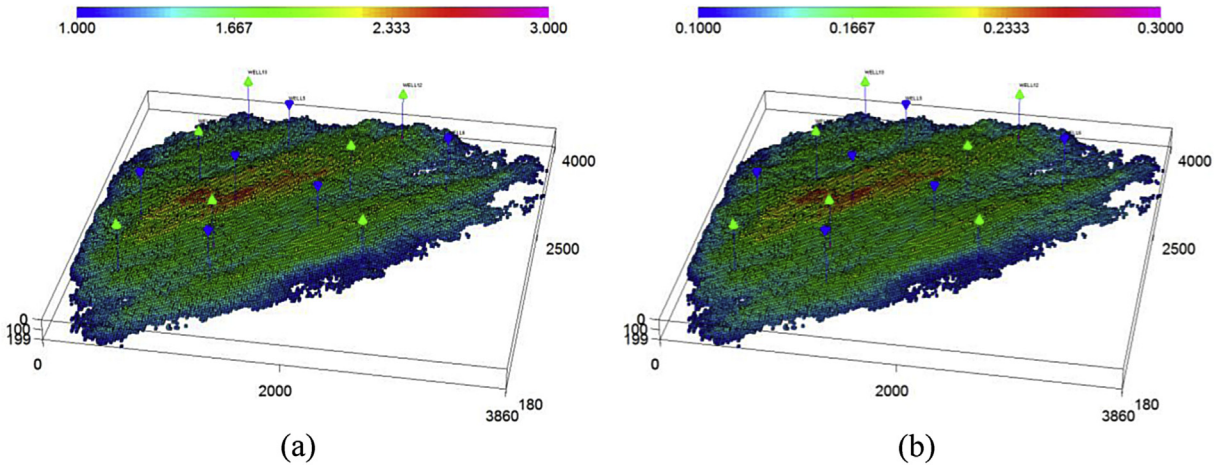

Fig. 16. Permeability distribution ($\times 10^{-13}\,m^2$) - case study 3. a) X and Y directions and b) Z direction.

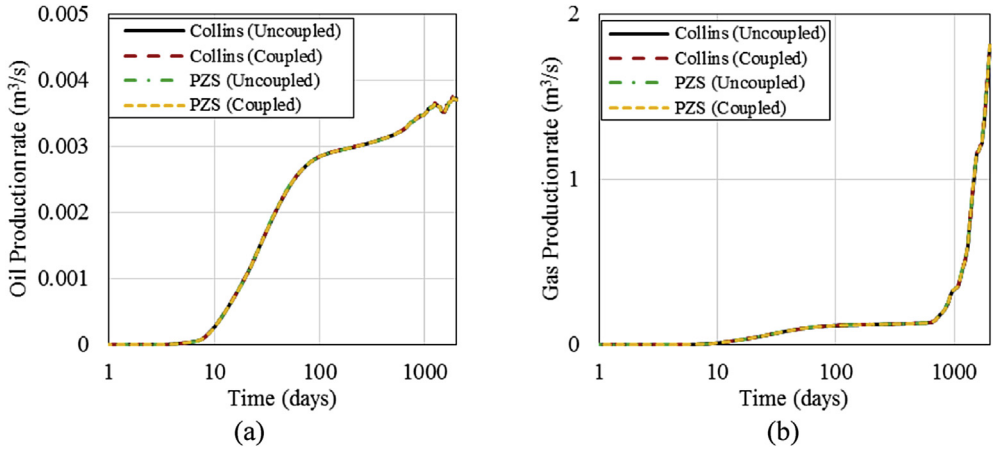

Fig. 18. Production rates - case study 3. a) Oil and b) gas.

The time-step profiles are presented in Fig. 7, where it can be observed that the FI approaches used, in average, a time-step twenty times bigger than the IMPEC approach. In fact, the FI approaches could use even larger time-steps, but it would reduce the solution accuracy in time. We can also verify that the two PZS formulations did not present cuts in time-steps as it is verified for Collins et al. (1992) formulation. The time-step cuts takes place when the Newton's method does not reduce the material balance residues enough or the changes in the primary variables do not converge. In this work, the maximum number of iterations per time-step is set to twenty. Once twenty Newton iterations are performed without successful convergence, the time-step is halved and restarted as a new time-step. This procedure is done until a time-step can achieve convergence. For this study, the time-step for the FI approaches was limited to 20 days, while the time-step for the IMPEC was limited to 1 day, in order to avoid the appearance of spurious oscillations.

Fig. 8 presents the highest Jacobian's condition number for each time-step obtained for each of the FI approaches. Such condition number is approximated computed using the options available in the PETSc package (Balay et al., 2013). From Fig. 8, we can verify that although the condition number for PZS formulation was larger than the Collins et al. (1992) formulation, it did not present large variation in the time-step history, and as it was verified before, the time-step for PZS was constant for most of the simulation. On the other hand, when the Collins et al. (1992) formulation presented a smaller condition number, the time-step was clearly reduced. At least for this first case study, such a behavior is a clear indication that the PZS has a better-condition Jacobian.

The gas saturation field at 2190 days of simulation is presented in Fig. 9. From this figure, it can be observed a good agreement between the fields obtained with all the different approaches.

The number of Newton iterations and the CPU times are presented in Table 5. It can be observed that the PZS approaches (coupled and uncoupled wells) are faster than both Collins et al. and the IMPEC formulation. It is possibly a result of the reduced number of Newton iterations required by the new formulation, the smaller size of linear system that is solved in each Newton iteration, a better - conditioned system. The average condition number and the number of iterations used by the solver are also presented in Table 5. We can verify from the results that in average the FI formulations presented similar number of iterations to solve the linear systems and the Collins et al. (1992) showed the smallest condition number, but is was due to the reduction in time-step that occurred several times during the simulation as it can be verified in Fig. 7.

The second case study refers to a gas/solvent injection performed by Killough and Kossack (1987). The fluid data is presented in Table 6. The reservoir permeability is heterogeneous in X, Y, and Z directions. The permeability field is presented in Fig. 10. For this study, only two wells are considered: one injector and one producer. Physical dispersion is also considered for this case. A 160 × 160 × 10 Cartesian grid is used for simulation of this case study. The reservoir data is presented in Table 7. Once again, the Stone II is used to model the relative permeability curves, with parameters given in Table 8.

The production rates are presented in a semi-log plot in Fig. 11.

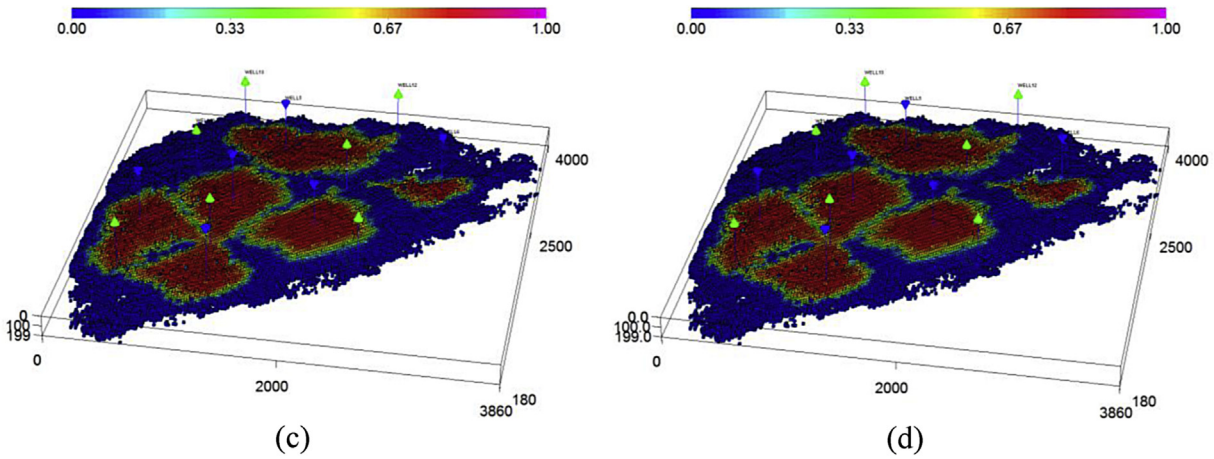

Fig. 19. CO_2 mole fraction field - case study 3 at 2000 days a) Collins et al. uncoupled with wells; b) Collins et al. with coupled wells; c) PZS with uncoupled wells; and d) PZS with coupled wells.

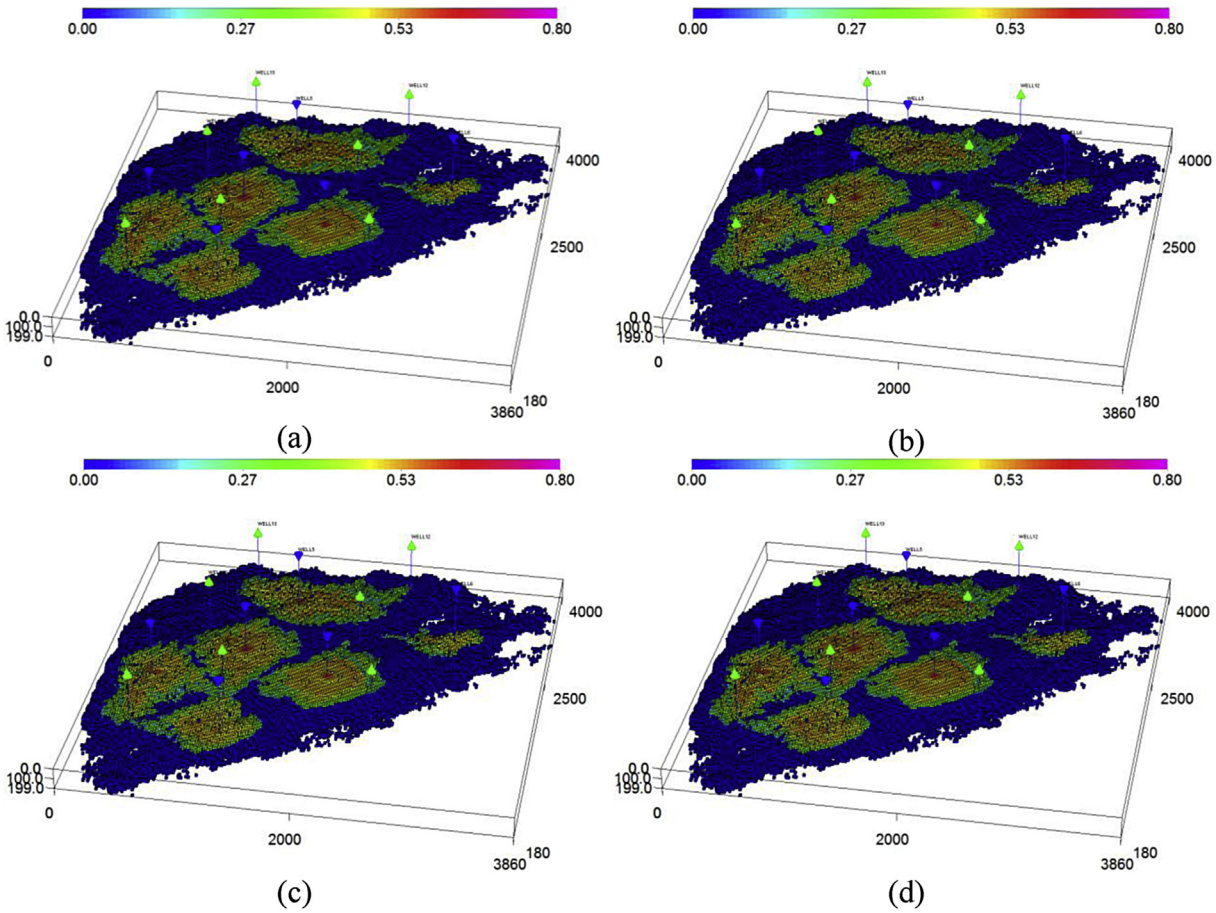

Fig. 20. Gas saturation field - case study 3 at 2000 days. a) Collins et al. with uncoupled wells; b) Collins et al. with coupled wells; c) PZS with uncoupled wells; and d) PZS with coupled wells.

From this figure, we can observe a good agreement for the production curves. It is worth to note that the PZS approach with coupled wells had a better match with the IMPEC solution. It is important to stress that due to time-step limitation of the IMPEC approach, the IMPEC solution is expected to be less prone to numerical dispersion. Therefore, from all FI solutions we may conclude that the PZS with coupled wells produced a more accurate solution for this case study.

A comparison of the gas saturation field at 1000 days is presented in Fig. 12, where a good agreement can be observed between all formulations tested.

As shown in Fig. 13, the time-step profile was very smooth, and reached the maximum value of 20 days; in order to be conservative and do not reduce the accuracy in time, the maximum time-step was fixed for all FI formulations. The maximum time-step for the IMPEC formulation was set to 0.005 days in order to avoid spurious oscillations in the production curves and simulation crash. Therefore, one can verify that the ratio between the time-step of the FI approaches compared to IMPEC approach was about 4000 times for this case study.

Fig. 14 presents the highest Jacobian's condition number for each time-step obtained for each of the FI approaches versus time. It can be observed that in general the PZS with coupled wells provided a smaller condition number. This is quite interesting since its results were also more accurate in time (closer to the IMPEC approach).

From Table 9, it can be observed that the FI formulations had a similar CPU time, but the fastest formulation was the PZS with coupled wells, although it produced more Newton iterations. The IMPEC formulation was about 27 times more expensive than the FI approaches presented here and it is not suitable for this case. It is worthwhile to mention that when dispersion is not considered, the time-steps obtained for the IMPEC formulation are largely increased, which allows a reasonable CPU time. The addition of dispersion, however, cut-down the time-steps and the CPU time is largely increased. The average maximum condition number and the total number of iterations performed by the solver are also presented in Table 9. Although, the difference between the average condition number were not large, the PZS presented the smallest condition number that was followed also by a smaller CPU time.

For the last case study, a grid with several inactive cells is presented. Herein, only the FI approaches are compared, once the IMPEC approach was not able to simulate this case. A $200 \times 200 \times 10$ grid is used with only 99,816 active cells. Thirteen wells are considered with 6 producers and 7 injectors. The absolute permeability, porosity and the grid shape is synthetic and was developed for testing the inactive cell approach for UTCOMPRS. Also, a second liquid hydrocarbon phase is formed in this

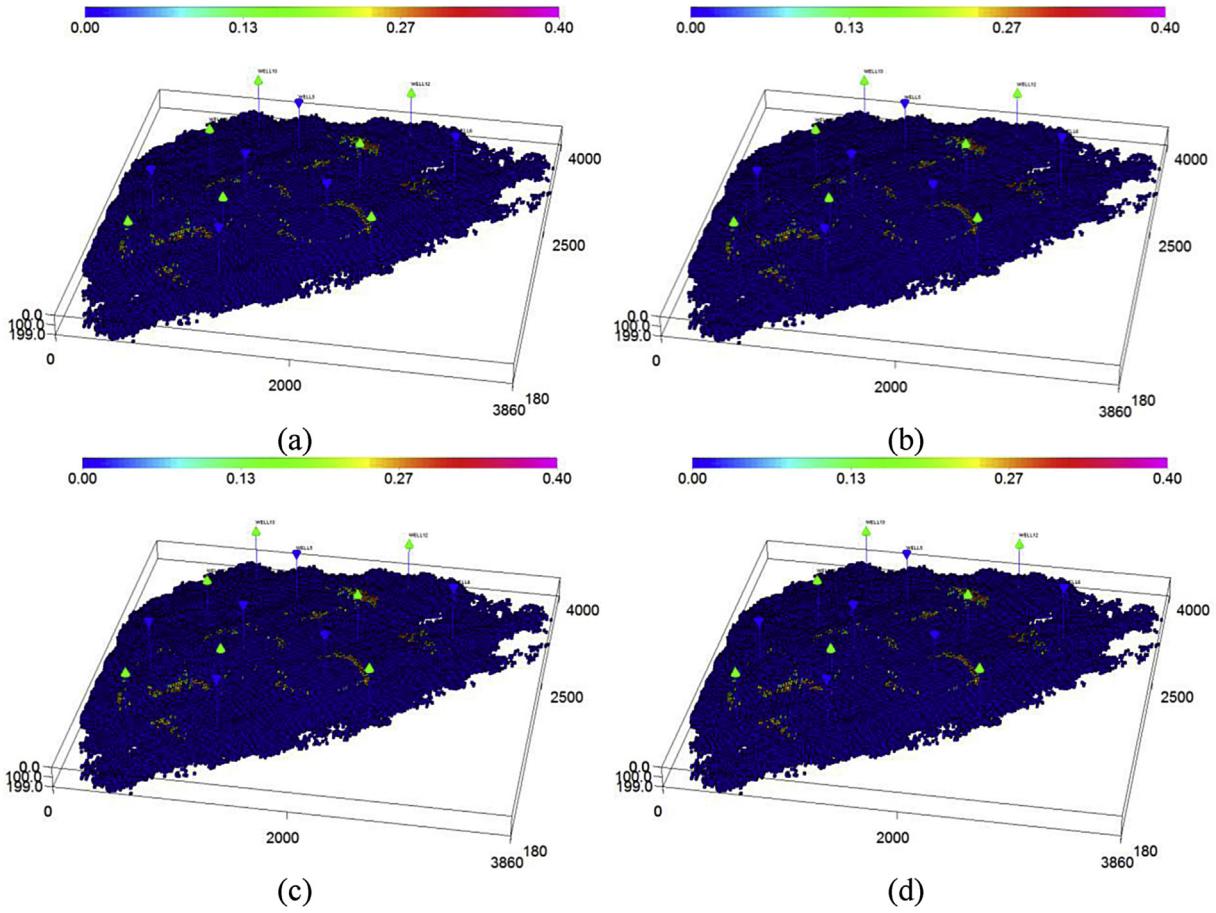

Fig. 21. Second liquid hydrocarbon saturation field - case study 3 at 2000 days. a) Collins et al. with uncoupled wells; b) Collins et al. with coupled wells; c) PZS with uncoupled wells; and d) PZS with coupled wells.

case. Therefore, a three phase flash calculation is used and a four phase flow takes place in some parts of the reservoir. This is also an important feature that is tested in this case with the new formulation. The data for the BSB west Texas Oil (Khan et al., 1992) is used, and it is presented in Table 10. The reservoir data is provided in Table 11. The Corey model (Corey, 1986) is used for the relative permeabilities and the parameters are presented in Table 12.

The reservoir depth from the top of the reservoir is presented in Fig. 15, where a view from the top is presented, as well as a view from the bottom of the reservoir. The permeability fields are presented in Fig. 16 and the porosity in Fig. 17.

The production curves are presented in Fig. 18. Once again, good match between the production curves is observed. The CO_2 mole fraction field, gas saturation field, and second liquid hydrocarbon saturation field at 2000 days are presented in Figs. 19–21, respectively. From these figures, we can verify a very good agreement between fields obtained with all the formulations tested.

The time-step profile for each formulation is presented in Fig. 22. The formulations have a very similar time-step profile. It is important to notice the large changes in time-step toward the end of simulation. This is believed to be caused by phase flipping close to the mixture critical point, which may cause issues on the time-step selection algorithm. However, such issue did not affect the production curves. Due to the complexity of this case, the condition number analysis will be omitted since approximating it was too challenging and the obtained values for condition number had no correlation at all with any performance parameter.

The CPU times and number of Newton iterations are presented in Table 13. We can observe that the PZS without coupled wells was the fastest approach for this case followed by Collins et al. formulation which was about 3% more expensive.

7. Conclusions

In this work, a new fully implicit formulation was proposed. The new formulation used pressure, water saturation, and overall composition as primary variables, all intensive variables. A procedure was presented to obtain the Jacobian for the new set of intensive variables using a formulation that was based on extensive primary variables.

The new formulation was tested and compared with the extensive formulation, which the new formulation derives from, and with the original IMPEC approach from UTCOMPRS simulator that has been benchmarked with commercial and in-house simulators along the past years. The case studies presented here show that the new formulation

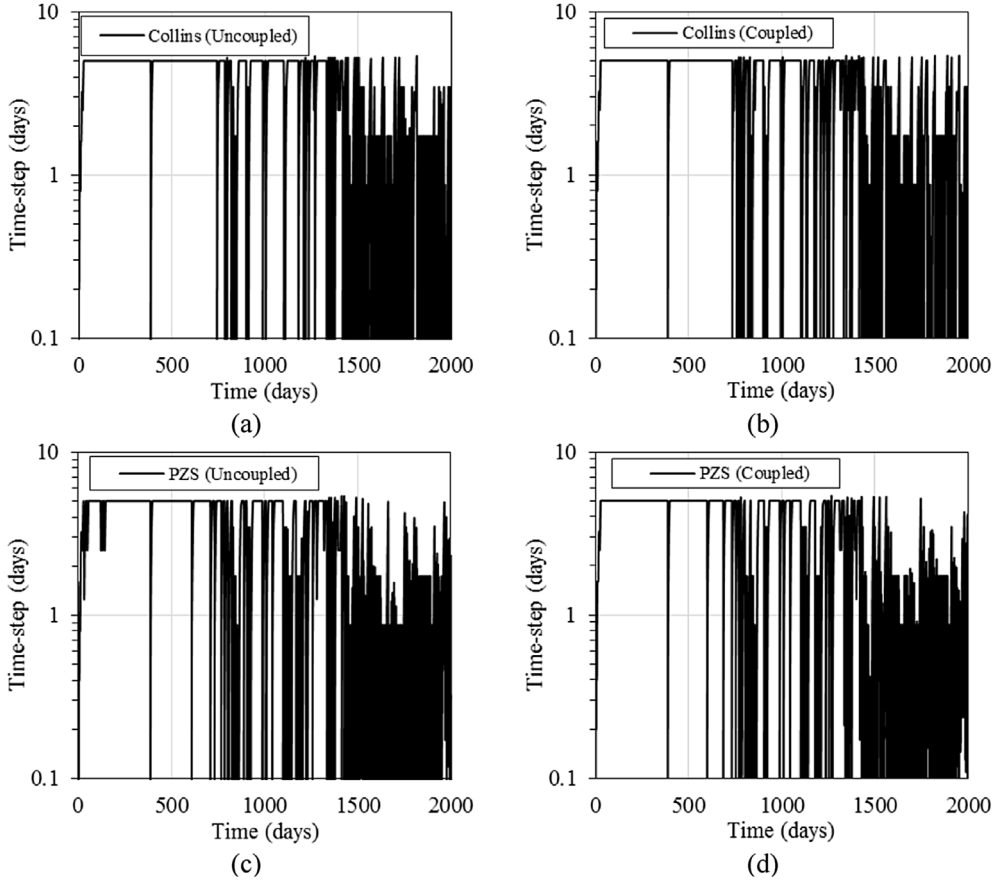

Fig. 22. Time-step profile - case study 3. a) Collins (uncoupled), b) Collins (coupled), c) PZS (uncoupled) and d) PZS (coupled).

Table 13
CPU Time and number of Newton iterations - Case 3.

Formulation	CPU Time (s)	Normalized CPU Time	Total number of Newton iterations
Collins et al. with uncoupled wells	100,353	1.03	4317
Collins et al. with coupled wells	113,146	1.16	4556
PZS with uncoupled wells	97,403	1.000	5065
PZS with coupled wells	104,747.	1.08	4964

is, in general faster, than the other mentioned approaches. Better performance was also observed for several other test cases that are not presented in this paper. Additionally, the new approach requires less storage than the previous original Collins et al. (1992) formulation. The new approach was also successful in simulating reservoirs with irregular geometries through the use of the inactive cells approach.

We can conclude that the formulation presented here is a powerful approach to speed up reservoir simulators, but more study is needed in order to determine what processes and features affect the performance of the implemented and tested formulations.

Acknownledgments

The first and second authors would like to acknowledge CNPq (The National Council for Scientific and Technological Development of Brazil) for its financial support through the grants 234476/2013-3 and 305851/2015-2, respectively.

Appendix A. Derivatives of phase compositions and phase mole fraction

We notice that several properties such as density, saturations, and viscosity are function of the phase composition and the phase mole fractions. Therefore, derivatives of the phase composition and phase mole fraction with respect to the number of moles of each component and pressure are required. The procedure that follows is based on the works of Subramanian et al. (1987) and Wong et al. (1987) and has been implemented by Fernandes (2014) and Fernandes et al. (2016).

The derivative of phase composition with respect to a primary variable X, pressure or total number of moles in this case, of a given component is written as

$$\frac{\partial x_{ij}}{\partial X} = \frac{\left(\frac{\partial n_{ij}}{\partial X}\sum_{l=1}^{n_c} n_{lj} - n_{ij}\sum_{l=1}^{n_c}\frac{\partial n_{lj}}{\partial X}\right)}{\left[\sum_{l=1}^{n_c} n_{lj}\right]^2}, \quad i = 1, \ldots, n_c, \; k = 1, \ldots, n_c, \; j = 2, \ldots, n_p, \tag{A.1}$$

and the phase mole fraction is obtained as

$$\frac{\partial L_j}{\partial X} = \frac{\left[\frac{\partial n_j}{\partial X}\sum_{l=2}^{n_p} n_l - n_j \sum_{l=2}^{n_p}\frac{\partial n_l}{\partial X}\right]}{\left(\sum_{l=2}^{n_p} n_l\right)^2}, \quad k = 1, \ldots, n_c, \quad j = 2, \ldots, n_p, \tag{A.2}$$

where

$$n_j = \sum_{l=1}^{n_c} n_{ij}, \quad \text{i= } 1, \ldots, n_c, \quad j = 2, \ldots, n_p. \tag{A.3}$$

Therefore, obtaining the derivatives of the number of moles of each component in each phase with respect with the primary variables is essential.

For two hydrocarbon phase equilibrium (i.e. oil-gas), the derivatives of n_{ij} with respect to pressure can be obtained by solving the following $n_c \times n_c$ linear system:

$$\begin{bmatrix} \frac{\partial \ln f_{1r}}{\partial n_{1r}} + \frac{\partial \ln f_{1j}}{\partial n_{1j}} & \cdots & \frac{\partial \ln f_{1r}}{\partial n_{nc r}} + \frac{\partial \ln f_{1j}}{\partial n_{nc j}} \\ \vdots & \ddots & \vdots \\ \frac{\partial \ln f_{nc r}}{\partial n_{1r}} + \frac{\partial \ln f_{ncj}}{\partial n_{1j}} & \cdots & \frac{\partial \ln f_{nc r}}{\partial n_{nc r}} + \frac{\partial \ln f_{ncj}}{\partial n_{nc j}} \end{bmatrix} \begin{bmatrix} \frac{\partial n_{1r}}{\partial P} \\ \vdots \\ \frac{\partial n_{nc r}}{\partial P} \end{bmatrix} = \begin{bmatrix} \frac{\partial \ln f_{1j}}{\partial P} - \frac{\partial \ln f_{1r}}{\partial P} \\ \vdots \\ \frac{\partial \ln f_{ncj}}{\partial P} - \frac{\partial \ln f_{nc r}}{\partial P} \end{bmatrix}, \tag{A.4}$$

where f_{ij} is the fugacity of component i in phase j and the subscripts r and j refer to the two hydrocarbon phases existent in a given grid-block; herein in this work, it could be oil-gas, oil-second liquid, and gas-second liquid. Observe that the solution of the system in Eq. (A.4) provides the derivatives of mole components in phase r. The derivatives for phase j are obtained as

$$\frac{\partial n_{sj}}{\partial P} = -\frac{\partial n_{sr}}{\partial P}, \qquad s = 1, \ldots, n_c, \tag{A.5}$$

For the derivatives with respect to the number of moles, n_c system of equations with n_c unknowns need to be solved. All the systems have the form

$$\begin{bmatrix} \frac{\partial \ln f_{1r}}{\partial n_{1r}} + \frac{\partial \ln f_{1j}}{\partial n_{1j}} & \cdots & \frac{\partial \ln f_{1r}}{\partial n_{nc r}} + \frac{\partial \ln f_{1j}}{\partial n_{nc j}} \\ \vdots & \ddots & \vdots \\ \frac{\partial \ln f_{nc r}}{\partial n_{1r}} + \frac{\partial \ln f_{ncj}}{\partial n_{1j}} & \cdots & \frac{\partial \ln f_{nc r}}{\partial n_{nc r}} + \frac{\partial \ln f_{ncj}}{\partial n_{nc j}} \end{bmatrix} \begin{bmatrix} \frac{\partial n_{1r}}{\partial N_k} \\ \vdots \\ \frac{\partial n_{nc r}}{\partial N_k} \end{bmatrix} = \begin{bmatrix} \frac{\partial \ln f_{1j}}{\partial n_{kj}} \\ \vdots \\ \frac{\partial \ln f_{ncj}}{\partial n_{kj}} \end{bmatrix}, \qquad k = 1, \ldots, n_c. \tag{A.6}$$

Once again, the solution of the n_c systems only provide solution for phase r, whereas the solution for phase j is obtained as follows:

$$\frac{\partial n_{sj}}{\partial N_k} = \delta_{sk} - \frac{\partial n_{sr}}{\partial N_k}, \qquad s = 1, \ldots, n_c; \qquad k = 1, \ldots, n_c. \tag{A.7}$$

where δ_{sk} is unity if $s=k$ and zero otherwise.

Similar procedure is performed for the three-phase equilibrium (oil-gas-second liquid). The derivatives with respect to pressure require a solution of a system with $2 \times n_c$ unknowns.

$$\begin{bmatrix} A_{11} & \cdots & A_{1n_c} \\ \vdots & \ddots & \vdots \\ A_{n_c 1} & \cdots & A_{n_c n_c} \end{bmatrix} \begin{bmatrix} X_1 \\ \vdots \\ X_{n_c} \end{bmatrix} = \begin{bmatrix} B_1 \\ \vdots \\ B_{n_c} \end{bmatrix}, \tag{A.8}$$

where

$$A_{is} = \begin{bmatrix} \frac{\partial \ln f_{io}}{\partial n_{so}} + \frac{\partial \ln f_{ig}}{\partial n_{sg}} & \frac{\partial \ln f_{ig}}{\partial n_{sg}} \\ \frac{\partial \ln f_{ig}}{\partial n_{sg}} & \frac{\partial \ln f_{ig}}{\partial n_{sg}} + \frac{\partial \ln f_{il}}{\partial n_{sl}} \end{bmatrix}; X_s = \begin{bmatrix} \frac{\partial n_{so}}{\partial P} \\ \frac{\partial n_{sl}}{\partial P} \end{bmatrix}; B_i = \begin{bmatrix} \frac{\partial \ln f_{ig}}{\partial P} - \frac{\partial \ln f_{io}}{\partial P} \\ \frac{\partial \ln f_{ig}}{\partial P} - \frac{\partial \ln f_{il}}{\partial P} \end{bmatrix}. \tag{A.9}$$

Herein, we obtain the derivatives of the moles of oil and second liquid phases. For the gas phase, the derivatives can be obtained as

$$\frac{\partial n_{sg}}{\partial P} = -\frac{\partial n_{so}}{\partial P} - \frac{\partial n_{sl}}{\partial P}, \qquad s = 1, \ldots, n_c. \tag{A.10}$$

Similarly, the derivatives with respect to the total number of moles of each component require the solution of n_c systems with $2 \times n_c$ unknowns.

$$\begin{bmatrix} A_{11} & \cdots & A_{1n_c} \\ \vdots & \ddots & \vdots \\ A_{n_c 1} & \cdots & A_{n_c n_c} \end{bmatrix} \begin{bmatrix} X_1^k \\ \vdots \\ X_{n_c}^k \end{bmatrix} = \begin{bmatrix} B_1^k \\ \vdots \\ B_{n_c}^k \end{bmatrix}, \qquad k = 1, \ldots, n_c, \tag{A.11}$$

with

$$A_{is} = \begin{bmatrix} \frac{\partial \ln f_{io}}{\partial n_{so}} + \frac{\partial \ln f_{ig}}{\partial n_{sg}} & \frac{\partial \ln f_{ig}}{\partial n_{sg}} \\ \frac{\partial \ln f_{ig}}{\partial n_{sg}} & \frac{\partial \ln f_{ig}}{\partial n_{sg}} + \frac{\partial \ln f_{il}}{\partial n_{sl}} \end{bmatrix}; X_s^k = \begin{bmatrix} \frac{\partial n_{so}}{\partial N_k} \\ \frac{\partial n_{sl}}{\partial N_k} \end{bmatrix}; B_i^k = \begin{bmatrix} \frac{\partial \ln f_{ig}}{\partial n_{kg}} \\ \frac{\partial \ln f_{ig}}{\partial n_{kg}} \end{bmatrix}, k = 1, \ldots, n_c. \tag{A.12}$$

Notice that the coefficient matrix does not change no matter if we are trying to obtain the derivatives with respect to pressure or moles. Again, the solution of the system provides the derivatives for the oil and second-liquid phases. For the gas phase, the derivatives can be obtained as

$$\frac{\partial n_{sg}}{\partial N_k} = \delta_{sk} - \frac{\partial n_{so}}{\partial N_k} - \frac{\partial n_{sl}}{\partial N_k}, \qquad s = 1, \ldots, n_c; \quad k = 1, \ldots, n_c. \tag{A.13}$$

The linear systems are solved using the Cholesky's decomposition. See Fernandes (2014) for details on how these equations are obtained.

References

Acs, G., Doleschall, S., Farkas, E., 1985. General Purpose compositional model. Soc. Petrol. Eng. J. 25, 543–553. https://doi.org/10.2118/10515-PA.

Araújo, A.L.S., Fernandes, B.R.B., Drumond Filho, E.P., Araujo, R.M., Lima, I.C.M., Gonçalves, A.D.R., Marcondes, F., Sepehrnoori, K., 2016. 3D compositional reservoir simulation in conjunction with unstructured grids. Braz. J. Chem. Eng. 33, 347–360. https://doi.org/10.1590/0104-6632.20160332s20150011.

Ayala, L.F., 2004. Compositional Modeling of Naturally-fractured Gas-condensate Reservoirs in Multi-mechanistic Flow Domains (PhD Dissertation). The Pennsylvania State University, State College, PA, USA.

Ayala, L.F., Ertekin, T., Adewumi, M.A., 2006. Compositional modeling of retrograde gas-condensate reservoirs in multimechanistic flow domains. SPE J. 11, 480–487. https://doi.org/10.2118/94856-PA.

Balay, S., Adams, M.F., Brown, J., Brune, P., Buschelman, K., Eijkhout, V., Gropp, W.D., Kaushik, D., Knepley, M.G., Mcinnes, L.C., Rupp, K., Smith, B.F., Zhang, H., 2013. PETSc User's Manual. Argonne National Laboratory, USA.

Baliga, B.R., Patankar, S.V., 1983. A control volume finite-element method for two-dimensional fluid flow and heat transfer. Numer. Heat Transf 6, 245–261. https://doi.org/10.1080/01495728308963086.

Branco, C.M., Rodriguez, F., 1996. A semi-implicit formulation for compositional reservoir simulation. SPE Adv. Technol. 4, 171–177. https://doi.org/10.2118/27053-PA.

Cao, H., 2002. DEVELOPMENT of TECHNIQUES for GENERAL PURPOSE SIMULATORS. PhD Dissertation. Stanford University, Stanford, USA.

Cao, H., Aziz, K., 2002. Performance of IMPSAT and impsat-aim models in compositional simulation. In: Presented at the SPE Annual Technical Conference and Exhibition. Society of Petroleum Engineers, San Antonio, USA. https://doi.org/10.2118/77720-MS.

Chang, Y., 1990. Development and Application of an Equation of State Compositional Simulator (PhD Dissertation). The University of Texas at Austin, USA.

Chang, Y., Pope, G.A., Sepehrnoori, K., 1990. A higher-order finite-difference compositional simulator. J. Petrol. Sci. Eng. 5, 35–50. https://doi.org/10.1016/0920-4105(90)90004-M.

Chien, M.C.H., Lee, S.T., Chen, W.H., 1985. A new fully implicit compositional simulator. In: Presented at the SPE Reservoir Simulation Symposium. Society of Petroleum Engineers, Dallas, TX, USA. https://doi.org/10.2118/13385-MS.

Coats, K.H., 1980. An equation of state compositional model. Soc. Petrol. Eng. J. 20, 363–376. https://doi.org/10.2118/8284-PA.

Collins, D.A., Nghiem, L.X., Li, Y.-K., Grabonstotter, J.E., 1992. An efficient approach to adaptive- implicit compositional simulation with an equation of state. SPE Reservoir Eng. 7, 259–264. https://doi.org/10.2118/15133-PA.

Corey, A.T., 1986. Mechanics of Immiscible Fluids in Porous media, second ed. Water Resources Publications, Littleton, Colorado, U.S.A.

Doroh, M.G., 2012. Development and Application of a Parallel Compositional Reservoir Simulator. Master Thesis. The University of Texas at Austin, Austin, USA.

Ewing, R.E., Russell, T.F., Young, L.C., 1989. An Anistropic Coarse-grid Dispersion Model of Heterogeneity and Viscous Fingering in Five-spot Miscible Displacement that Matches Experiments and Fine-Grid Simulations. Society of Petroleum Engineers, Houston, USA. https://doi.org/10.2118/18441-MS.

Fernandes, B.R.B., 2014. Implicit and Semi-implicit Techniques for the Compositional Petroleum Reservoir Simulation Based on Volume Balance. Master Thesis. Federal University of Ceara, Fortaleza, Brazil.

Fernandes, B.R.B., Drumond Filho, E.P., Gonçalves, A.D.R., Marcondes, F., Sepehrnoori, K., 2014a. Investigation of cross derivatives in corner point grids formulation in conjunction with compositional reservoir simulation. In: XXXV Iberian Latin-american Congress on Computational Methods in Engineering. Presented at the XXXV Iberian Latin-american Congress on Computational Methods in Engineering. ABMEC, Fortaleza, Brazil.

Fernandes, B.R.B., Gonçalves, A.D.R., Drumond Filho, E.P., da Costa Menezes Lima, I., Marcondes, F., Sepehrnoori, K., 2015a. A 3D total variation diminishing scheme for compositional reservoir simulation using the element-based finite-volume method. Numer. Heat Transf. Part Appl. 67, 839–856. https://doi.org/10.1080/10407782.2014.949196.

Fernandes, B.R.B., Lima, I.C.M., Araújo, A.L.S., Marcondes, F., Sepehrnoori, K., 2012. 2D compositional reservoir simulation using unstructured grids in heterogeneous reservoirs. In: Blucher Mechanical Engineering Proceedings, 1. Presented at the 10th World Congress on Computational Mechanics, Blucher, São Paulo, Brazil, pp. 1455–1474. https://doi.org/10.5151/meceng-wccm2012-18433.

Fernandes, B.R.B., Marcondes, F., Sepehrnoori, K., 2016. Comparison of two volume balance fully implicit approaches in conjunction with unstructured grids for compositional reservoir simulation. Appl. Math. Model. 40, 5153–5170. https://doi.org/10.1016/j.apm.2015.09.002.

Fernandes, B.R.B., Marcondes, F., Sepehrnoori, K., 2015b. Sequential implicit approach for compositional reservoir simulation in conjunction with unstructured grids. In: 23rd ABCM International Congress of Mechanical Engineering. Presented at the COBEM 2015. ABCM, Rio de Janeiro, Brazil. https://doi.org/10.20906/CPS/COB-2015-2688.

Fernandes, B.R.B., Marcondes, F., Sepehrnoori, K., 2013. Investigation of several interpolation functions for unstructured meshes in conjunction with compositional reservoir simulation. Numer. Heat Transf. Part Appl. 64, 974–993. https://doi.org/10.1080/10407782.2013.812006.

Fernandes, B.R.B., Sepehrnoori, K., Marcondes, F., 2017. A natural variable fully implicit compositional reservoir simulation. In: CILAMCE 2017. Presented at the CILAMCE 2017, . https://doi.org/10.20906/CPS/CILAMCE2017-0447.

Fernandes, B.R.B., Varavei, A., Marcondes, F., Sepehrnoori, K., 2014b. Comparison of an impec and a semi-implicit formulation for compositional reservoir simulation. Braz. J. Chem. Eng. 31, 977–991. https://doi.org/10.1590/0104-6632.20140314s00003084.

Fussell, L.T., Fussell, D.D., 1979. An iterative technique for compositional reservoir models. Soc. Pet. Eng. J. 19, 211–220. https://doi.org/10.2118/6891-PA.

Gharbi, R.B.C., 1989. Numerical Simulation of Unstable Displacements. Master's Thesis. The University of Texas at Austin, Austin, USA.

Haukas, J., Aavatsmark, I., Espedal, M., Reiso, E., 2007a. A new IMPSAT formulation for compositional simulation. In: Presented at the SPE Reservoir Simulation Symposium. Society of Petroleum Engineers, Houston, USA. https://doi.org/10.2118/106235-MS.

Haukas, J., Aavatsmark, I., Espedal, M., Reiso, E., 2007b. A comparison of two different IMPSAT models in compositional simulation. SPE J. 12, 145–151. https://doi.org/10.2118/101700-PA.

Kazemi, H., Vestal, C.R., Shank, D.G., 1978. An efficient multicomponent numerical simulator. Soc. Petrol. Eng. J. 18, 355–368. https://doi.org/10.2118/6890-PA.

Khan, S.A., Pope, G.A., Sepehrnoori, K., 1992. Fluid characterization of three-phase CO2/oil mixtures. In: Presented at the SPE/DOE Enhanced Oil Recovery Symposium. Society of Petroleum Engineers, Tulsa, Oklahoma, USA. https://doi.org/10.2118/24130-MS.

Killough, J.E., Kossack, C.A., 1987. Fifth comparative solution project: evaluation of miscible flood simulators. In: Presented at the SPE Symposium on Reservoir Simulation. Society of Petroleum Engineers, San Antonio, Texas. https://doi.org/10.2118/16000-MS.

Krueger, C.A., 1989. Numerical Simulator and Modeling of Viscous Fingering. Master Thesis. The University of Texas at Austin, Austin, USA.

Lacroix, S., Vassilevski, Y.V., Wheeler, M.F., 2000. Iterative Solvers of the Implicit Parallel Accurate Reservoir Simulator (IPARS). I: Single Processor Case (Technical Report No. 00–28). TICAM.

Liu, J., Delshad, M., Pope, G.A., Sepehrnoori, K., 1994. Application of higher-order flux-limited methods in compositional simulation. Transport Porous Media 16, 1–29. https://doi.org/10.1007/BF01059774.

Maliska, C.R., 2004. Computation Heat Transfer and Fluid Mechanics. Livros Tecnicos e Cientificos, Rio de Janeiro.

Marcondes, F., Sepehrnoori, K., 2010. An element-based finite-volume method approach for heterogeneous and anisotropic compositional reservoir simulation. J. Petrol. Sci. Eng. 73, 99–106. https://doi.org/10.1016/j.petrol.2010.05.011.

Mehra, R.K., Heidemann, R.A., Aziz, K., 1983. An accelerated successive substitution algorithm. Can. J. Chem. Eng. 61, 590–596. https://doi.org/10.1002/cjce.5450610414.

Michelsen, M.L., 1982. The isothermal flash problem. Part I. Stability. Fluid Phase Equil. 9, 1–19. https://doi.org/10.1016/0378-3812(82)85001-2.

Nghiem, L.X., Fong, D.K., Aziz, K., 1981. Compositional modeling with an equation of state (includes associated papers 10894 and 10903). Soc. Petrol. Eng. J. 21, 687–698. https://doi.org/10.2118/9306-PA.

Peaceman, D.W., 1983. Interpretation of well-block pressures in numerical reservoir simulation with nonsquare grid blocks and anisotropic permeability. Soc. Petrol. Eng. J. 23, 531–543. https://doi.org/10.2118/10528-PA.

Peaceman, D.W., 1978. Interpretation of well-block pressures in numerical reservoir simulation. Soc. Pet. Eng. J. 18, 183–194. https://doi.org/10.2118/6893-PA.

Peng, D.-Y., Robinson, D.B., 1976. A new two-constant equation of state. Ind. Eng. Chem. Fundam. 15, 59–64. https://doi.org/10.1021/i160057a011.

Perschke, D.R., 1988. Equation of State Phase Behavior Modelling for Compositional Simulator. PhD Dissertation. The University of Texas at Austin, USA.

Perschke, D.R., Chang, Y., Pope, G.A., Sepehrnoori, K., 1989a. Comparison of Phase Behavior Algorithms for an Equation-of-state Compositional Simulator.

Perschke, D.R., Pope, G.A., Sepehrnoori, K., 1989b. Phase Identification during Compositional Simulation.

Quandalle, P., Savary, D., 1989. An Implicit in Pressure and Saturations Approach to Fully Compositional Simulation. Presented at the SPE Symposium on Reservoir Simulation. Society of Petroleum Engineers, Houston, USA. https://doi.org/10.2118/18423-MS.

Saad, Y., Schultz, M.H., 1986. GMRES: a generalized minimal residual algorithm for solving nonsymmetric linear systems. SIAM J. Sci. Stat. Comput. 7, 856–869. https://doi.org/10.1137/0907058.

Santos, L.O.S., Marcondes, F., Sepehrnoori, K., 2013a. A 3D compositional miscible gas flooding simulator with dispersion using Element-based Finite-Volume method. J. Petrol. Sci. Eng. 112, 61–68. https://doi.org/10.1016/j.petrol.2013.10.004.

Santos, L.O.S., Varavei, A., Sepehrnoori, K., 2013b. A Comparison of Various Formulations for Compositional Reservoir Simulation. Society of Petroleum Engineers, The Woodlands, Texas, USA. https://doi.org/10.2118/163630-MS.

Spillette, A.G., Hillestad, J.G., Stone, H.L., 1973. A High-stability Sequential Solution Approach to Reservoir Simulation. Presented at the Fall Meeting of the Society of Petroleum Engineers of AIME. Society of Petroleum Engineers, Las Vegas, NV, USA. https://doi.org/10.2118/4542-MS.

Stone, H.L., 1973. Estimation of three-phase relative permeability and residual oil data. J. Can. Pet. Technol. 12. https://doi.org/10.2118/73-04-06.

Subramanian, G., Trangenstein, J.A., Mochizuki, S., Shen, E.-C., 1987. Efficient fluid behavior computations in a sequential compositional reservoir simulator. In: SPE Symposium on Reservoir Simulation. Presented at the SPE Symposium on Reservoir Simulation. Society of Petroleum Engineers, San Antonio, Texas, USA. https://doi.org/10.2118/16024-MS.

Trangenstein, J.A., 1987. Customized minimization techniques for phase equilibrium computations in reservoir simulation. Chem. Eng. Sci. 42, 2847–2863. https://doi.org/10.1016/0009-2509(87)87051-3.

Wang, P., Yotov, I., Wheeler, M., Arbogast, T., Dawson, C., Parashar, M., Sepehrnoori, K., 1997. A new generation EOS compositional reservoir simulator: Part I - formulation and discretization. In: Presented at the SPE Reservoir Simulation Symposium. Society of Petroleum Engineers, Dallas, USA. https://doi.org/10.2118/37979-MS.

Watts, J.W., 1986. A compositional formulation of the pressure and saturation equations. SPE Reservoir Eng. 1, 243–252. https://doi.org/10.2118/12244-PA.

Wong, T.W., Aziz, K., 1989. Considerations in the development of multipurpose reservoir simulation models. In: Presented at the First and Second International Forum on Reservoir Simulation.

Wong, T.W., Firoozabadi, A., Nutakki, R., Aziz, K., 1987. A comparison of two approaches to compositional and black oil simulation, in: SPE symposium on reservoir simulation. In: Presented at the SPE Symposium on Reservoir Simulation. Society of Petroleum Engineers. https://doi.org/10.2118/15999-MS.

Young, L.C., 1990. Use of dispersion relationships to model adverse-mobility-ratio miscible displacements. SPE Reservoir Eng. 5, 309–316. https://doi.org/10.2118/14899-PA.

Young, L.C., Stephenson, R.E., 1983. A generalized compositional approach for reservoir simulation. Soc. Petrol. Eng. J. 23, 727–742. https://doi.org/10.2118/10516-PA.

Zhang, M., Ayala, L.F., 2018. A semi-analytical solution to compositional flow in liquid-rich gas plays. Fuel 212, 274–292. https://doi.org/10.1016/j.fuel.2017.08.097.

Zhang, M., Ayala, L.F., 2016. Analytical study of flowing and in-situ compositions in unconventional liquid-rich gas plays. In: SPE Annual Technical Conference and Exhibition. Presented at the SPE Annual Technical Conference and Exhibition. Society of Petroleum Engineers, Dubai, UAE. https://doi.org/10.2118/181567-MS.